NAVAL POSTGRADUATE SCHOOL
MONTEREY, CALIFORNIA

THESIS

NUMERICAL AND EXPERIMENTAL STUDY
OF FAILURE OF THE HUMAN PROXIMAL
FEMUR

by

Ronald R. Van Court

March 1996

Thesis Advisor: Young W. Kwon

Approved for public release; distribution is unlimited.

REPORT DOCUMENTATION PAGE

Public reporting burden for this collection of information is estimated to average 1 hour per response, including the time for reviewing instruction, searching existing data sources, gathering and maintaining the data needed, and completing and reviewing the collection of information. Send comments regarding this burden estimate or any other aspect of this collection of information, including suggestions for reducing this burden, to Washington Headquarters Services, Directorate for Information Operations and Reports, 1215 Jefferson Davis Highway, Suite 1204, Arlington, VA 22202-4302, and to the Office of Management and Budget, Paperwork Reduction Project (0704-0188) Washington DC 20503.

1. AGENCY USE ONLY *(Leave blank)*	2. REPORT DATE March 1996	3. REPORT TYPE AND DATES COVERED Master's Thesis

4. TITLE AND SUBTITLE NUMERICAL AND EXPERIMENTAL STUDY OF FAILURE OF THE HUMAN PROXIMAL FEMUR		5. FUNDING NUMBERS
6. AUTHOR(S): Van Court, Ronald R.		

7. PERFORMING ORGANIZATION NAME(S) AND ADDRESS(ES) Naval Postgraduate School Montcrey, CA 93943-5000	8. PERFORMING ORGANIZATION REPORT NUMBER

9. SPONSORING/MONITORING AGENCY NAME(S) AND ADDRESS(ES) Naval National Medical Center Department of Orthopedic Surgery 8901 Wisconsin Ave. Bethesda, MD 20889-5000	10. SPONSORING/MONITORING AGENCY REPORT NUMBER

11. SUPPLEMENTARY NOTES The views expressed in this thesis are those of the author and do not reflect the official policy or position of the Department of Defense or the U.S. Government.

12a. DISTRIBUTION/AVAILABILITY STATEMENT Approved for public release; distribution is unlimited.	12b. DISTRIBUTION CODE

13. ABSTRACT *(maximum 200 words)*

Static and dynamic experiments were conducted to study the failure loads and fracture patterns of human proximal femur bones, that are intact and core drilled. This was done to assist orthopedic surgeons better understand the effects of core drilling into the femoral head to remove osteonecrosis. Unlike pervious studies, where only static tests were conducted, dynamic tests were preformed to better simulate a lateral fall. A Finite Element Analysis (FEA) was also completed to understand stress distributions in the proximal femur when subjected to static and dynamic loads. Previous FEA models of the femur analyzed static loads only with just a core drilled hole at the lesser trochanter. This FEA model examines various sizes of hole diameters and locations on the greater trochanter as well as having the model loaded statically and dynamically.

14. SUBJECT TERMS Biomechanics, Femur, Proximal Femur, Osteonecrosis			15. NUMBER OF PAGES 74
			16. PRICE CODE

17. SECURITY CLASSIFICATION OF REPORT Unclassified	18. SECURITY CLASSIFICATION OF THIS PAGE Unclassified	19. SECURITY CLASSIFICATION OF ABSTRACT Unclassified	20. LIMITATION OF ABSTRACT UL

NUMERICAL AND EXPERIMENTAL STUDY OF FAILURE OF THE HUMAN PROXIMAL FEMUR

Ronald R. Van Court
Lieutenant, United States Navy
B.S., University of Arizona, 1989

Submitted in partial fulfillment
of the requirements for the degree of

MASTER OF SCIENCE IN MECHANICAL ENGINEERING

from the

NAVAL POSTGRADUATE SCHOOL

iv

ABSTRACT

Static and dynamic experiments were conducted to study the failure loads and fracture patterns of human proximal femur bones, that are intact and core drilled. This was done to assist orthopedic surgeons better understand the effects of core drilling into the femoral head to remove osteonecrosis. Unlike previous studies, where only static tests were conducted, dynamic tests were preformed to better simulate a lateral fall. A Finite Element Analysis (FEA) was also completed to understand stress distributions in the proximal femur when subjected to static and dynamic loads. Previous FEA models of the femur analyzed static loads only with just a core drilled hole at the lesser trochanter. This FEA model examines various sizes of hole diameters and locations on the greater trochanter as well as having the model loaded statically and dynamically.

TABLE OF CONTENTS

ACKNOWLEDGEMENTS

I would like to extend sincere thanks and gratitude to Professor Young W. Kwon for his guidance and assistance in the performance of this research. I would also like to thank my parents, Robert and Nancy, for years of support, love and belief in me. Finally, I would like to express my deepest appreciation and love to my wife, Monica and children, Robert and Jessica for their patience, understanding and love.

x

I. INTRODUCTION

Of the more than 250,000 hip fracture that occur each year, in both the civilian and military communities, approximately 3,300 of them are the result of osteonecrosis (bone disease) of the femoral head [Ref. 1 and 2].

Osteonecrosis is typically located in the anterior superior of the femur head and starts with constriction of the blood vessels in the femoral head. This constriction causes increased pressure and cuts off oxygen supply to the femoral head, killing that portion of the bone. As a result, net trabecular bone weakness will occur, and small fractures and/or trabecular collapse can be seen in the infracted region [Ref. 3]. The cancellous stiffness and strength can decrease by 50 to 70 percent [Ref. 4 and 5]. Thus, as trabecular is continually subjected to repetitive loads, such as walking, the necrotic region becomes more vulnerable to fatigue failure and/or to macroscopic fracture and collapse. If a collapse of the femoral head should occur a total hip replacement would be required. The fact that this disease is common in people as young as 30 years old presents special problems. A hip replacement in a 30 year old can be expected to last only seven years as a result of their high activity level. Subsequently, hip replacement would necessitate more bone removal with each replacement thus further surgery would be impossible by age 55, leaving the patient wheelchair bond.

Hip replacement, fortunately, can often be avoided by early intervention. One technique is core drilling, literally drilling out the diseased bone. However, when drilling a hole into the proximal femur, substantial load bearing material is temporarily lost until the bone grows back. This regrowth can take as long as six months. This treatment, therefore, raises several questions regarding the possibility of fracture following treatment. Currently, biomechanical testing of the

1

proximal femur has applied a static load to cause brakeage of the femur [Ref. 6 and 7]. This involves an instron or universal testing machine to apply a load to the superior margin of the femur head and record failure load.

In conjunction with Lt. Robert Blotter, MC, USNR a orthopedic surgeon at Naval Hospital, in Oakland, California, a new dynamic impact test equipment was used to simulate a lateral fall of the greater trochanter to study failure loads and fracture patterns of both intact and core drilled femurs. The scope of this research will address issues on data obtained from this impact testing and compare it to numerical data obtained from a three dimensional finite element model. To the authors best knowledge, this is the first dynamic testing of femurs to investigate their failure. This should serve to augment the existing data from static testing.

II. SPECIMEN PREPARATION

Sixteen human fresh frozen proximal femurs were used in this research; nine intact and seven core drilled. The donors were ten males and six females, ranging in age from 28 to 88 years old (average age 57.0 years). All donors died of natural causes with no trauma or disease of the femur bone.

All femur bones were examined to confirm no trauma and no disease. The bones were cut at mid-femur and were frozen at -15 degrees C. They were removed from the freezer the night before testing and prepared the morning of the test. Preparation included the cut end of each femur bone was potted in a 2.5 inch PVC pipe with methylmethacrylate (Figure 1). Seven femurs were core drilled from the lesser trochanter to the femoral head with a ten millimeter drill bit (Figure 2).
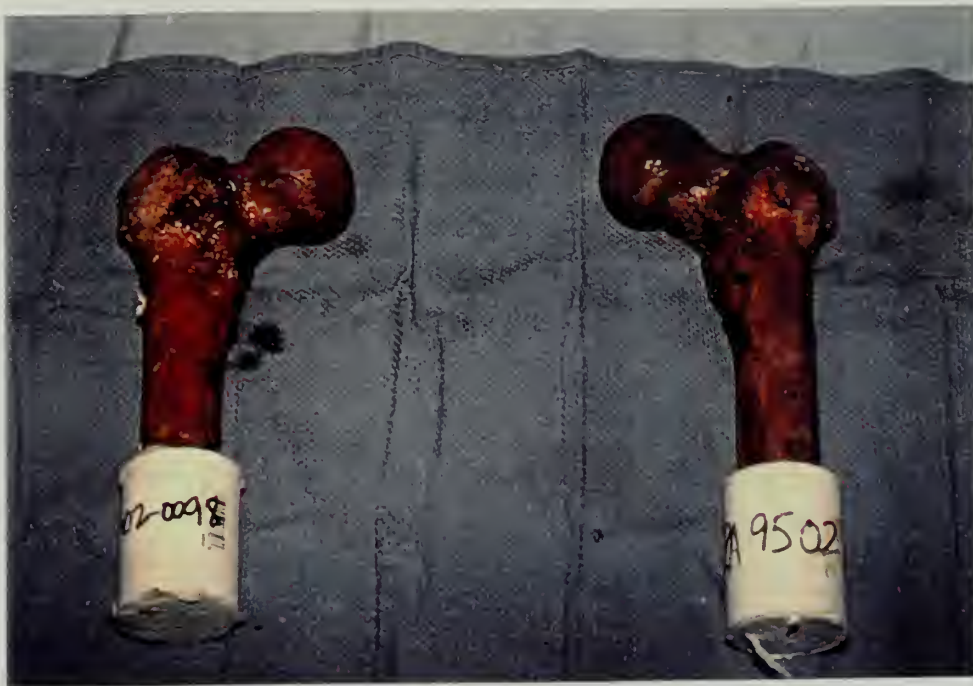
Figure 1: Femurs Potted in PVC Piping.

Figure 2: Core Drilling at the Lesser Trochanter.

4

III. TEST EQUIPMENT

To form a comparison with dynamic test results, six femurs were statically fractured using a universal testing machine. Of the six femurs, four were from males and two from females, ages 49 to 86 years old (average 61.2). Four of the femurs were core drilled and two were left intact. The femurs were placed vertically into a dividing head to adjust the femur to ten degrees of adduction to simulate the position in the body. A polyethylene cup was attached at the cross-head of the universal testing machine to distribute the load at the superior margin of the femoral head (Figures 3). Loads were applied to the femur at a rate of twenty millimeters per minute and the failure loads and fracture patterns were recorded and tabulated (Table 1).


Figure 3: Femur in Universal Testing Machine.

Femur	Core Drilled (10mm)	Age (Years)	Sex	Failure Load (N)	Fracture Pattern
1	No	54	Male	8451	Inter-trochanteric
2	No	52	Male	9563	Inter-trochanteric
3	Yes	86	Male	4314	Inter-trochanteric
4	Yes	49	Male	5606	Inter-trochanteric
5	Yes	50	Female	1112	Inter-trochanteric
6	Yes	76	Female	667	Inter-trochanteric

Table 1. Static Results.

To no surprise the static data suggests femurs that were core drilled failed at a substantially lesser load than intact femurs. The data also suggests that all femurs, core drilled or intact, would exhibit an intertrochanteric fracture (Figure 4). Because the static testing did not account for individual differences in femurs, a more realistic simulation was needed. Matched femurs were needed and were to be broken in a dynamic test phase.
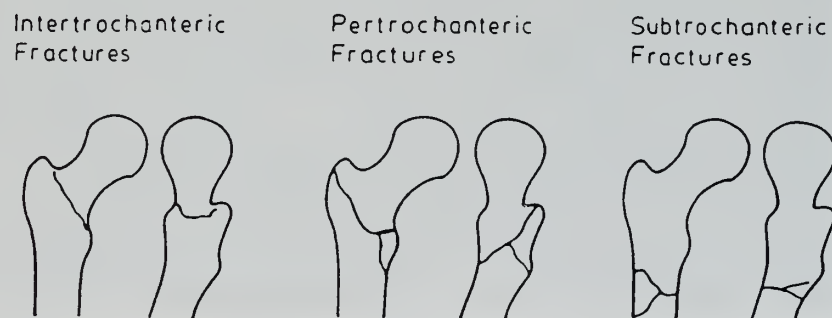
Figure 4: Types of Proximal Femur Fractures [Ref. 8].

The ten remaining femurs were fractured dynamically to better simulate a lateral fall. Of the ten, six were paired yielding three matched sets and four unpaired femurs. The seven donors were five males and two females ranging in age from 28 to 88 years old (average age 54.1 years). One femur from each matched set was core drilled and the remaining femurs, as well as the four unpaired, were intact. As previously stated, dynamic impact testing of femurs is unique in the literature, therefore a test stand had to be developed (Figure 5). To accurately simulate a lateral fall, the distal femur was again placed in ten degrees of adduction by inserting the distal end into a pillow block; a concave plexiglass plate covered the greater trochanter to evenly distribute the load (Figure 6). The femoral head was placed in a concave cup located at the base under a PCB 20,000 pound load cell on the impact stand. The load cell was attached to a 32 pound sled on guide rails approximately one meter above the greater trochanter of the femur.

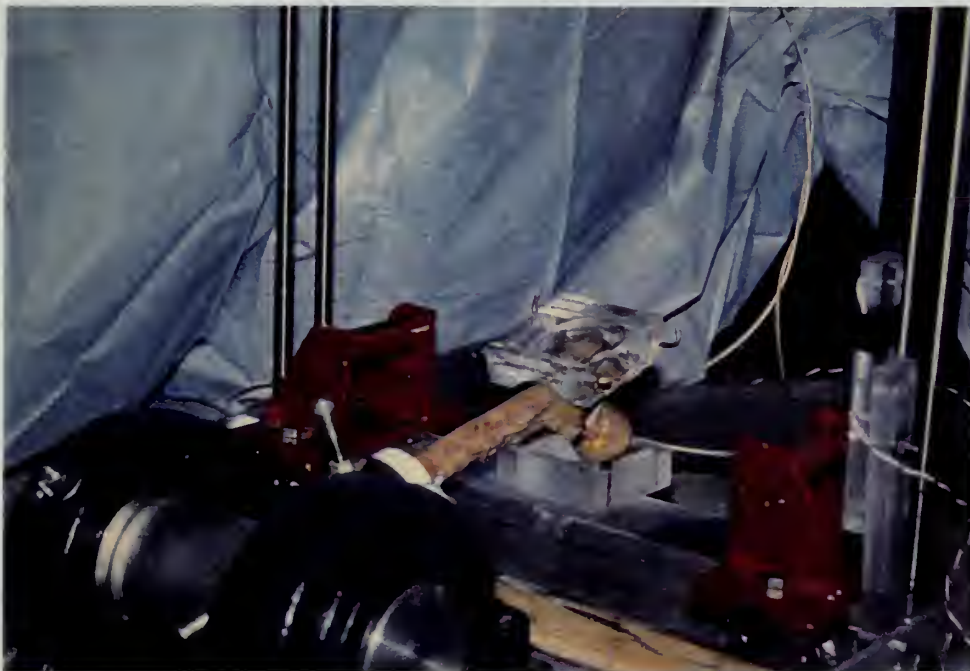Figure 5: Dynamic Impact Stand.

Figure 6: Femur in Dynamic Impact Stand.

This load cell was connected to an IBM 5151 computer via a PCB industrial teflon cable. When the sled was released, it slid along the guide rails to impact the greater trochanter. Just before the load cell impacted the greater trochanter and broke the femur, the sled struck a timing trigger to start the computer for data acquisition. The computer provided a raw output graph with voltage along the y-axis and time along the x-axis. This raw voltage had to be converted into a force (newton) using a calibration formula provided by PCB:

$$Force = \frac{10,000 x Voltage}{4.4482} \qquad (1)$$

Using this calibration formula, a simple Matlab code was generated to produce a force versus time graph (Figures 7-16).
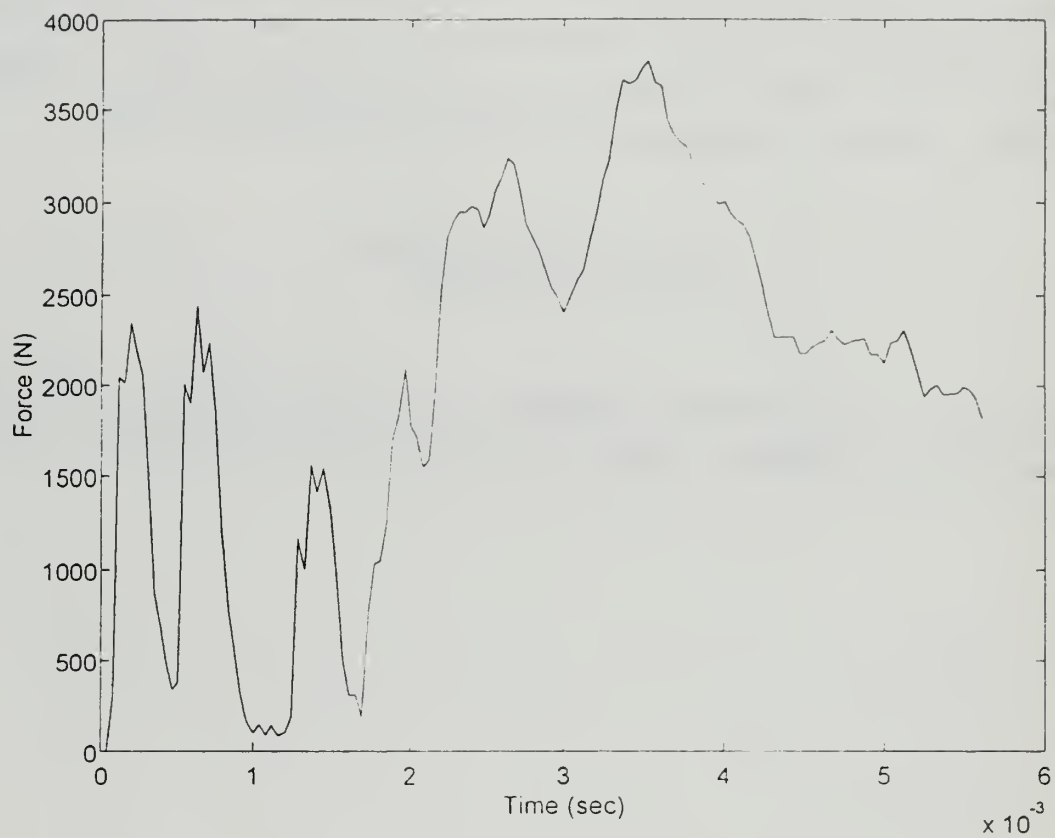
Figure 7: Force vs. Time for Femur 7, Intact (62 Year Old Male).
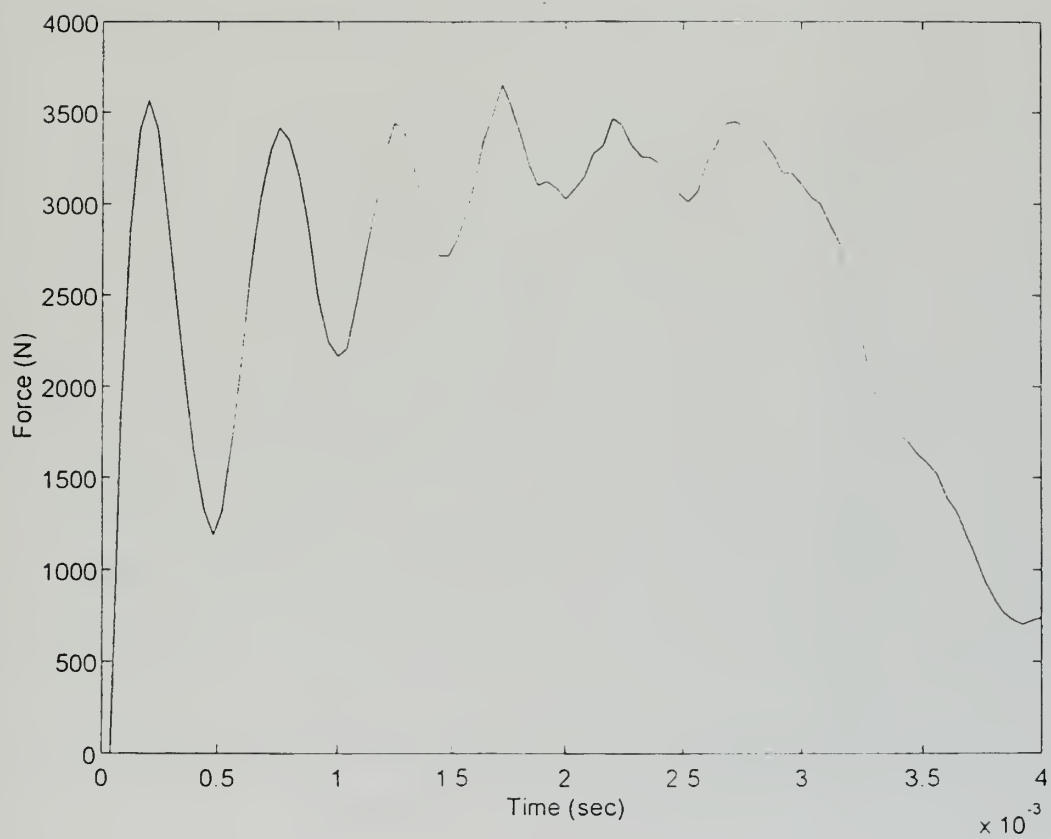
Figure 8: Force vs. Time for Force vs. Time for Femur 7A,
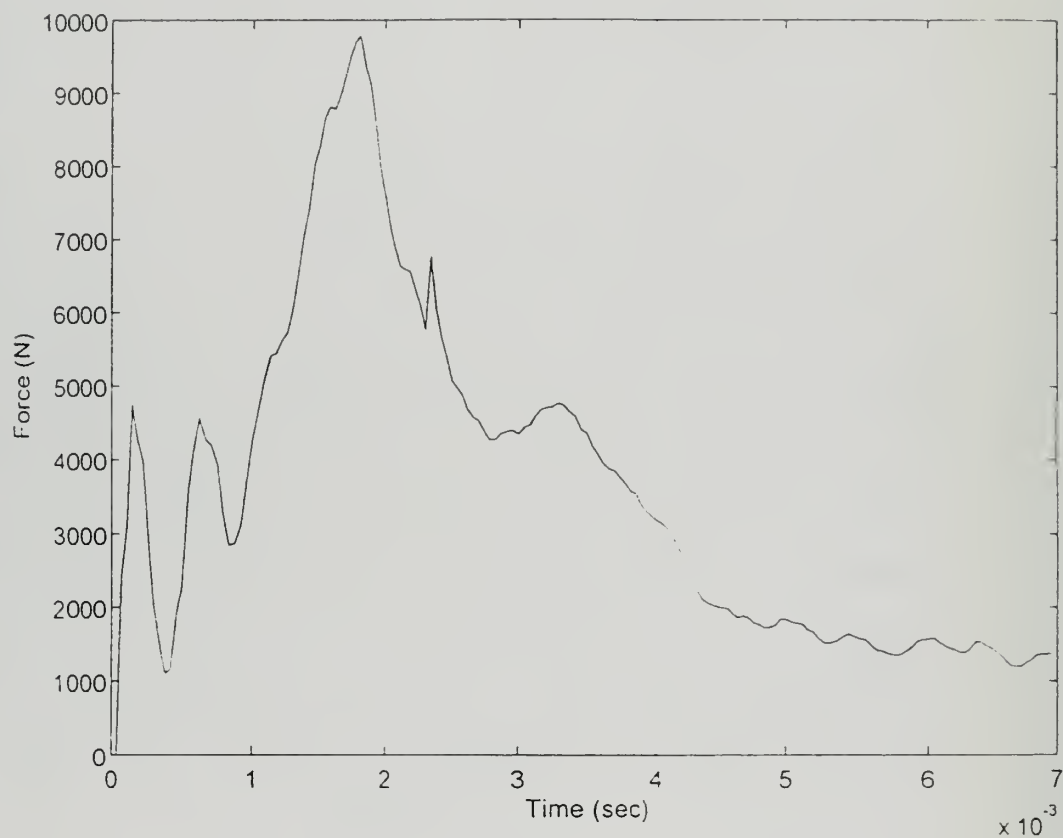Core Drilled (62 Year Old Male).

11

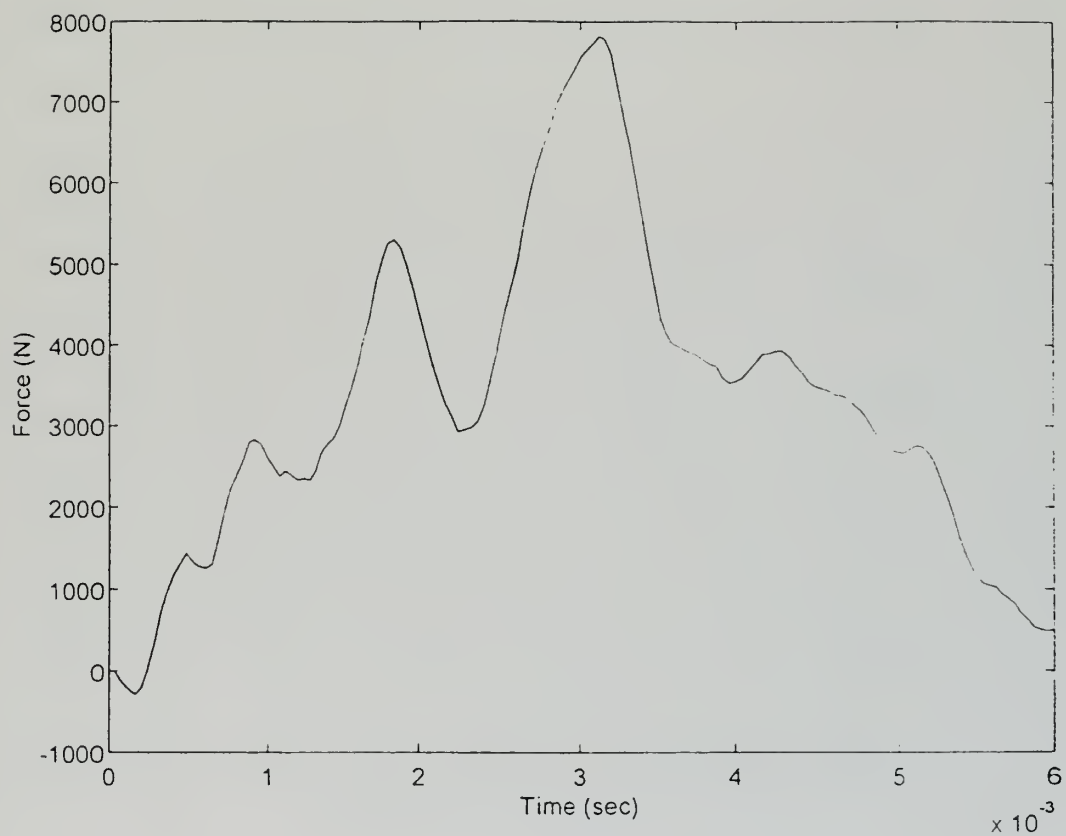Figure 9:   Force vs. Time for Femur 8, Intact (45 Year Old
Male).

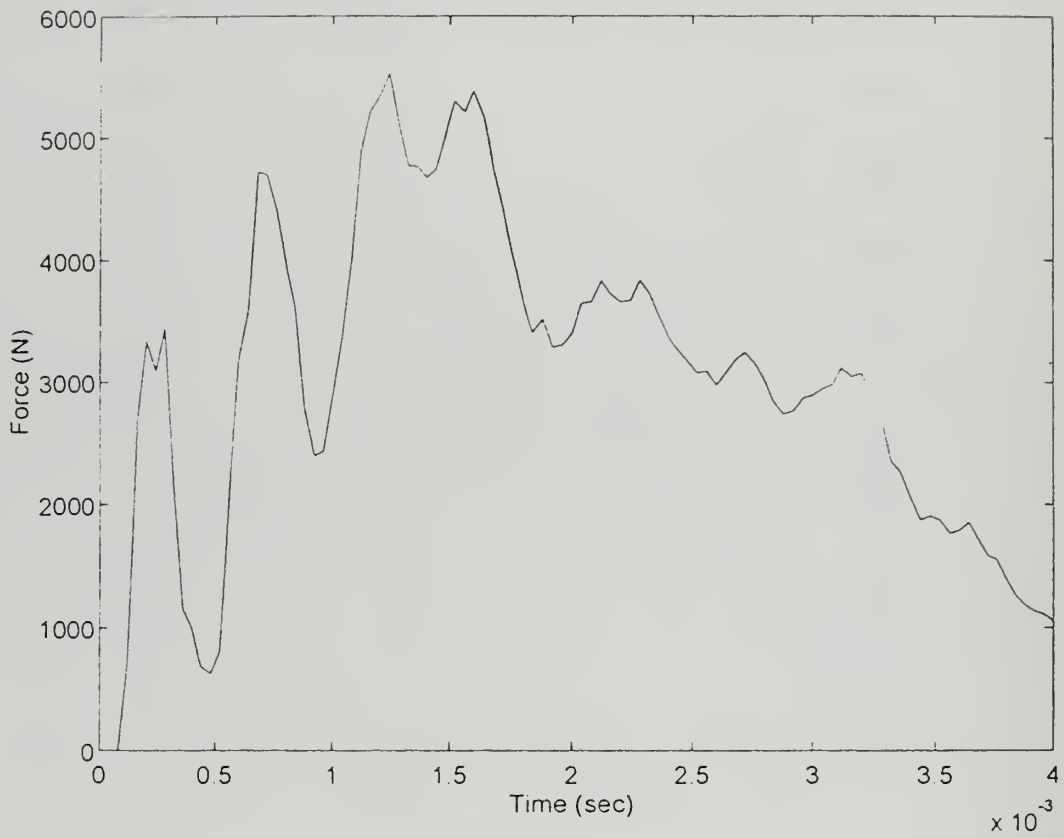Figure 10: Force vs. Time for Femur 8A, Core Drilled (45 Year Old Male).

13

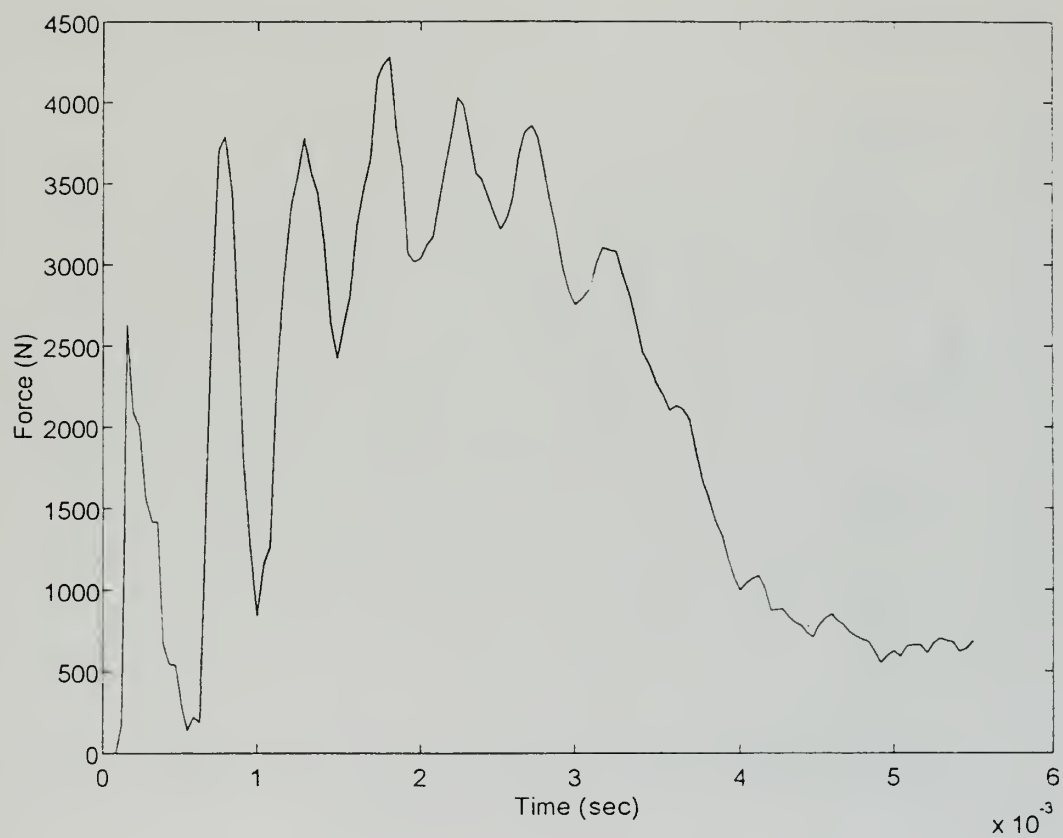Figure 11:   Force vs. Time for Femur 9, Intact (28 Year Old Female).

14

Figure 12: Force vs. Time for Femur 9A, Core Drilled (28 Year Old Female).
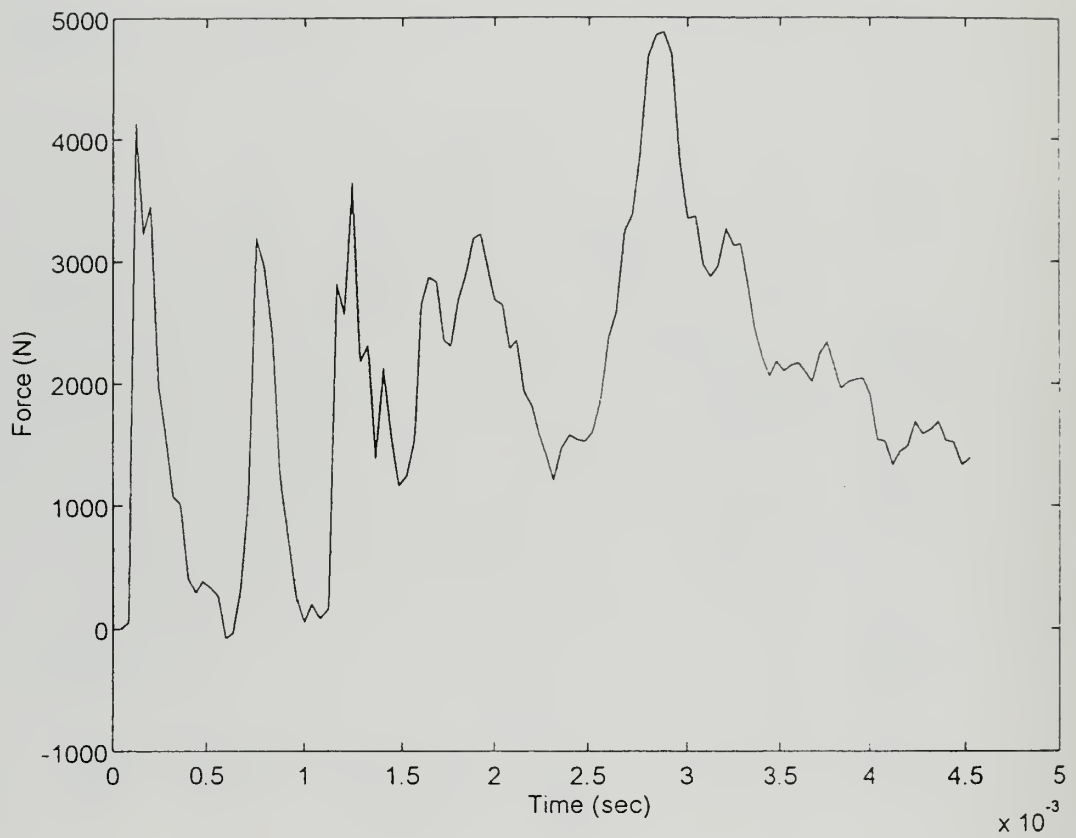
15

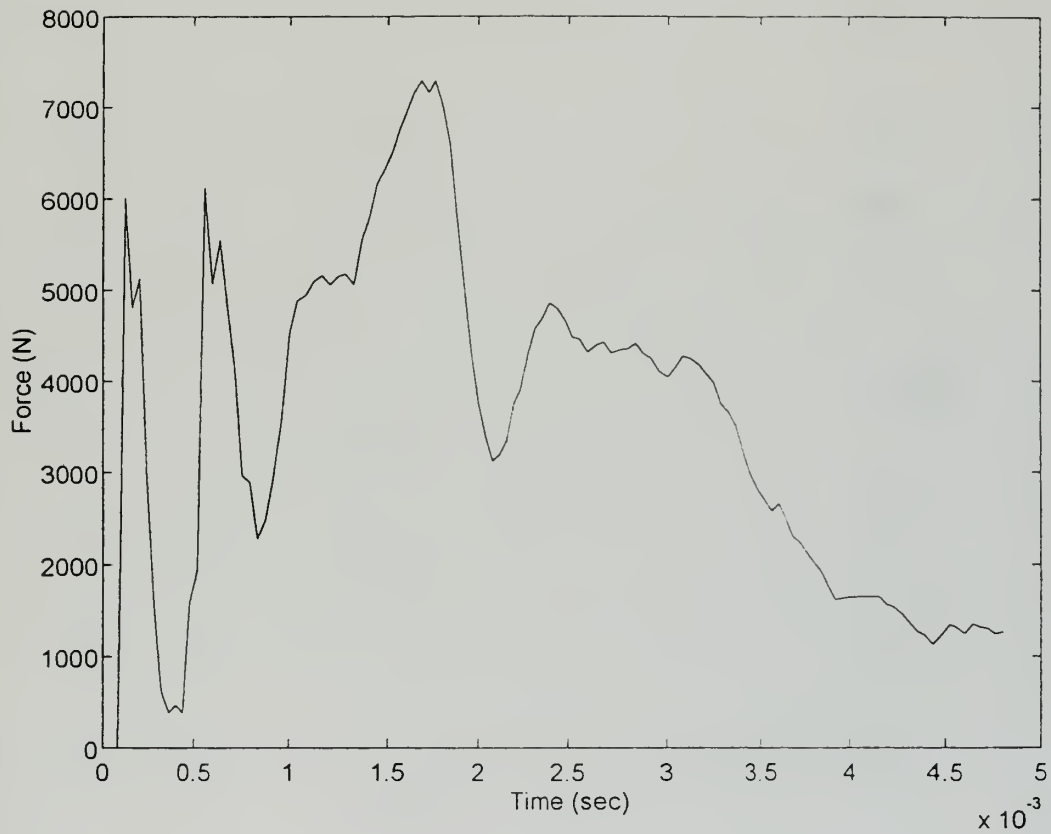**Figure 13: Force vs. Time for Femur 10, Intact (67 Year Old Male).**

Figure 14: Force vs. Time for Femur 11, Intact (60 Year Old Female).
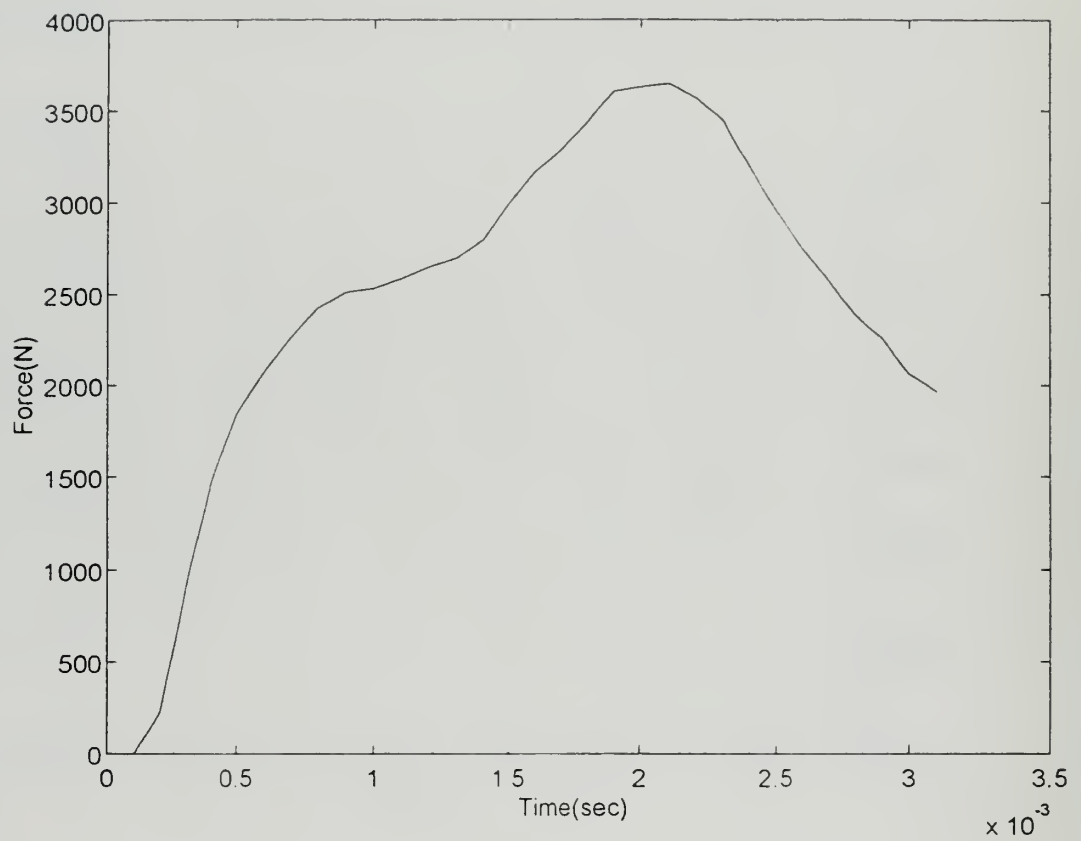
17

Figure 15: Force vs. Time for Femur 12, Intact (88 Year Old Male).
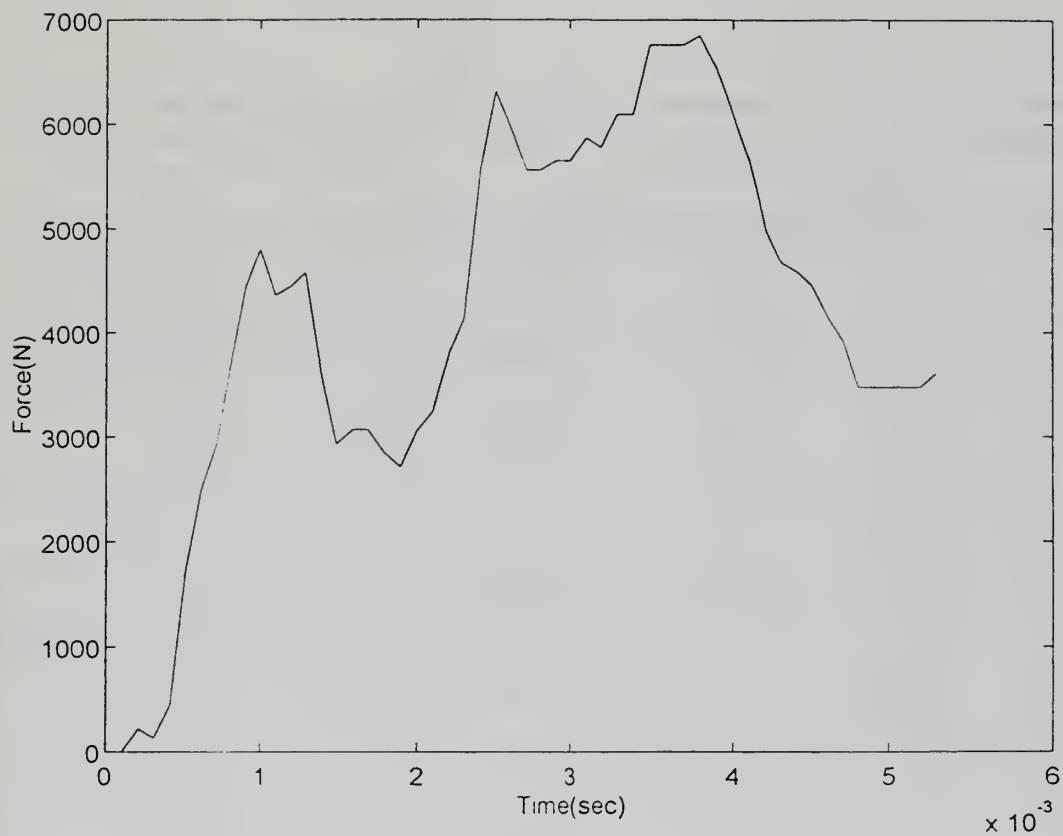
Figure 16: Force vs. Time for Femur 13, Intact (67 Year Old Male).

The highest peak on each graph represents the failure load of the femur. The smaller peaks are the vibrations of the relatively light (32 pound) sled striking the plexiglass plate on the greater trochanter. It is interesting to note that the entire time of the event is about six milliseconds. The failure loads and fracture patterns of the ten femurs were recorded and tabulated (Table 2).

Femur	Core Drilled (10mm)	Age (Years)	Sex	Failure Load (N)	Fracture Pattern
7	No	62	Male	3750	Sub-trochanteric
7A	Yes	62	Male	3500	Inter-trochanteric
8	No	45	Male	9900	Sub-trochanteric
8A	Yes	45	Male	7900	Inter-trochanteric
9	No	28	Female	5500	Per-trochanteric
9A	Yes	28	Female	4300	Inter-trochanteric
10	No	67	Male	4900	Sub-trochanteric
11	No	60	Female	7300	Per-trochanteric
12	No	88	Male	3600	Sub-trochanteric
13	No	60	Male	6700	Sub-trochanteric

Table 2. Dynamic Results.

The dynamic data shows that core drilled femurs fail at lower loads than intact femurs. This is not as surprising as the fracture patterns: All of the core drilled femurs exhibited intertrochanteric fractures following dynamic testing (Figure 17). However, of the intact femurs, five exhibited subtrochanteric fractures and two had pertrochanteric fractures (Figure 18). None had intertrochanteric fracture patterns. Recall in the static testing phase, both intact and core drilled femurs demonstrated intertrochanteric fractures.

Figure 17: Intertrochanteric Fracture.

Figure 18: Subtrochanteric Fracture.

22

IV. NUMERICAL MODELING

A finite element model of the femur bone was built and analyzed using I-DEAS from Structural Dynamics Research Corporation [Ref. 9]. The first step in creating the model was using a molded casting of a human proximal femur mapped out in cylindrical coordinates on a Mitutoyo coordinate machine. The cylindrical data points were then converted to cartesian data points and inputted into I-DEAS. The computer model was built in the simulation application by manually entering in the data points. Once the model was generated a shell mesh was built around the femur. Physical and material properties of the femur were then defined and various boundary and loading conditions were applied to the models. Static and dynamic stresses were solved for using linear static and normal mode dynamics (Lanczos Method), respectively. Using the information from the static and dynamic solutions, stress distributions were investigated.

A. MAPPING AND SOLID MODELING

A dividing head was used to secure the femur in place and allow for rotation of the bone for cylindrical coordinate mapping. The Mitutoyo coordinate machine was used to perform the mapping and was zeroed out at the center of the dividing head's clamps (Figure 19). The bone was secured at the femoral head, rather than at the shaft, in order to ensure there would be a single circular plane (Figure 20).
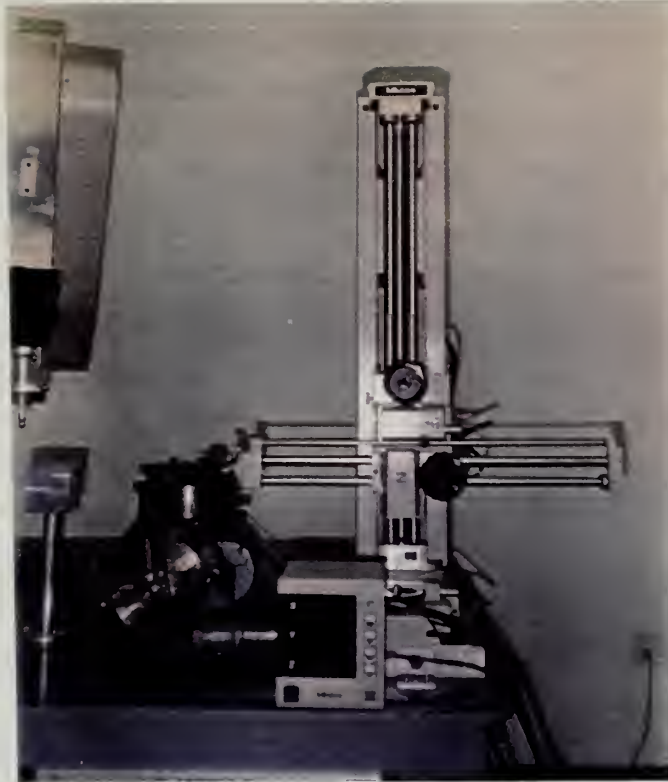
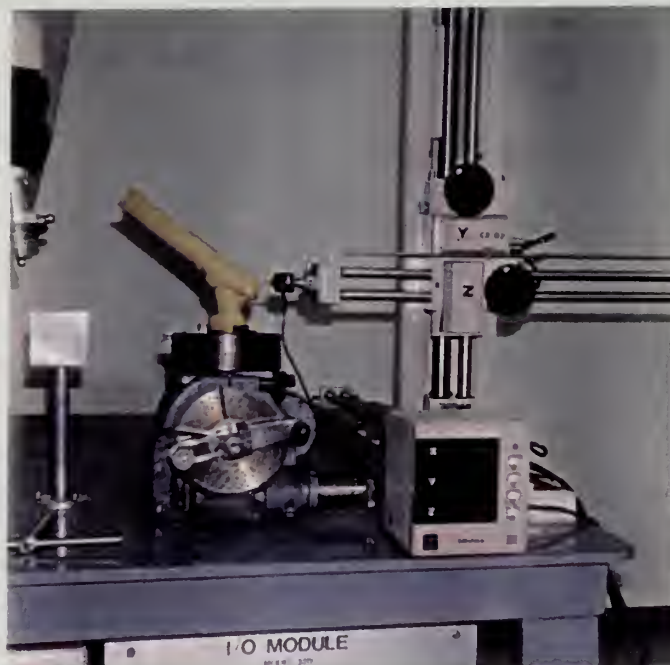Figure 19: Mitutoyo Coordinate Machine.

Figure 20: Femur Secured in the Dividing Head.

The femur was rotated completely, in ten degree increments in order to obtain a radial distance at each increment thus creating a circular plane. The coordinate machine's probe was raised in five millimeter increments creating twenty-two circular planes. The cylindrical data points were converted into cartesian data points utilizing simple math equations. Each cartesian data point for a circular plane was manually entered in I-DEAS using the spline function. The workplane was adjusted in the Z-direction upon completion of each circular plane (Figure 21). When the twenty-two planes were completed, the loft function was utilized to connect the planes and show the outside shell of the femur (Figure 22). Four other models were created in the same fashion except holes were bored into the femur. Two models had holes bored at the lesser trochanter, one at 10 millimeters in diameter and the other at 12 millimeters. The other two models had holes of the same diameter but located at the greater trochanter. These holes were cut using the extrude function (Figure 23 and 24).
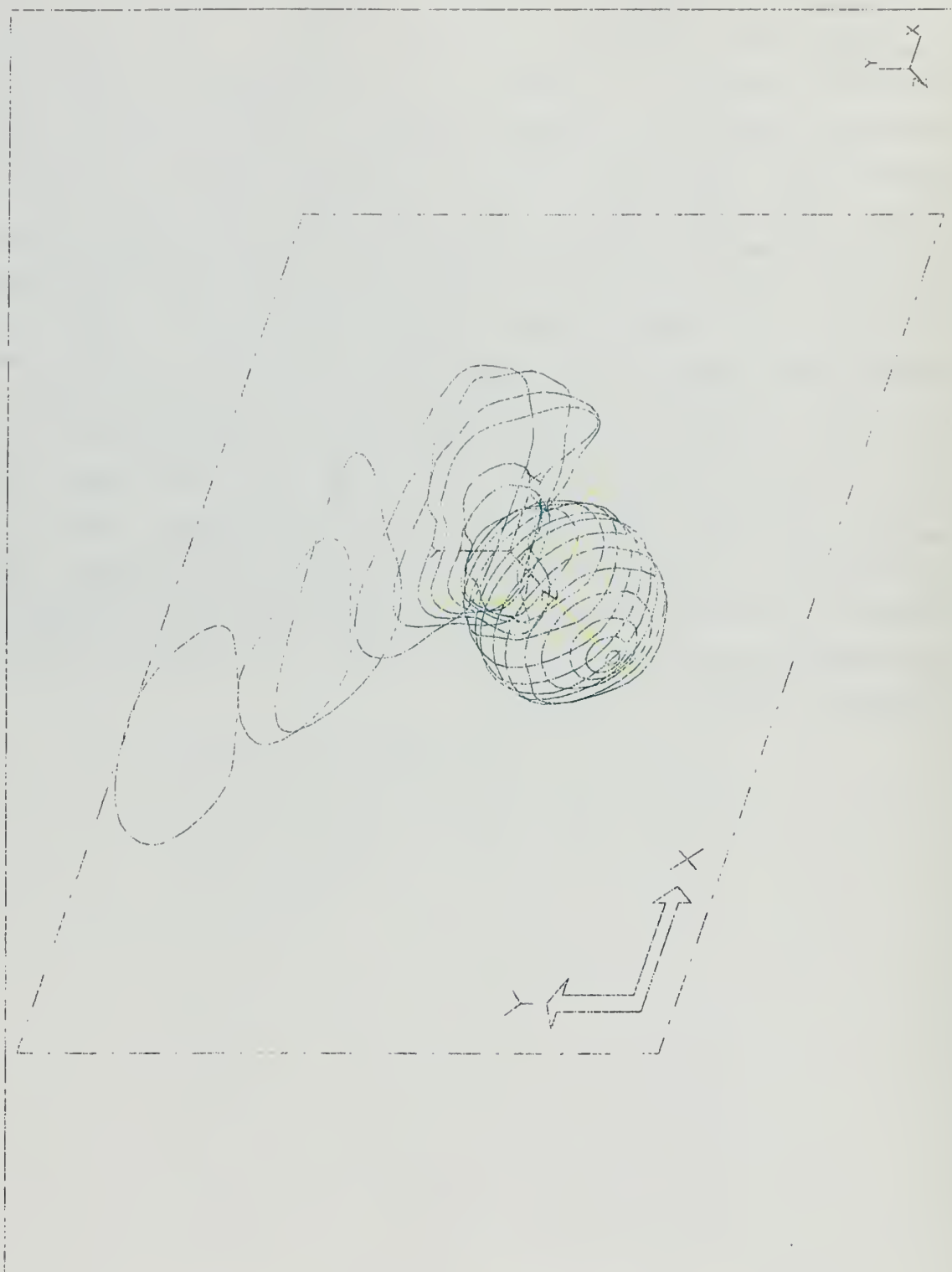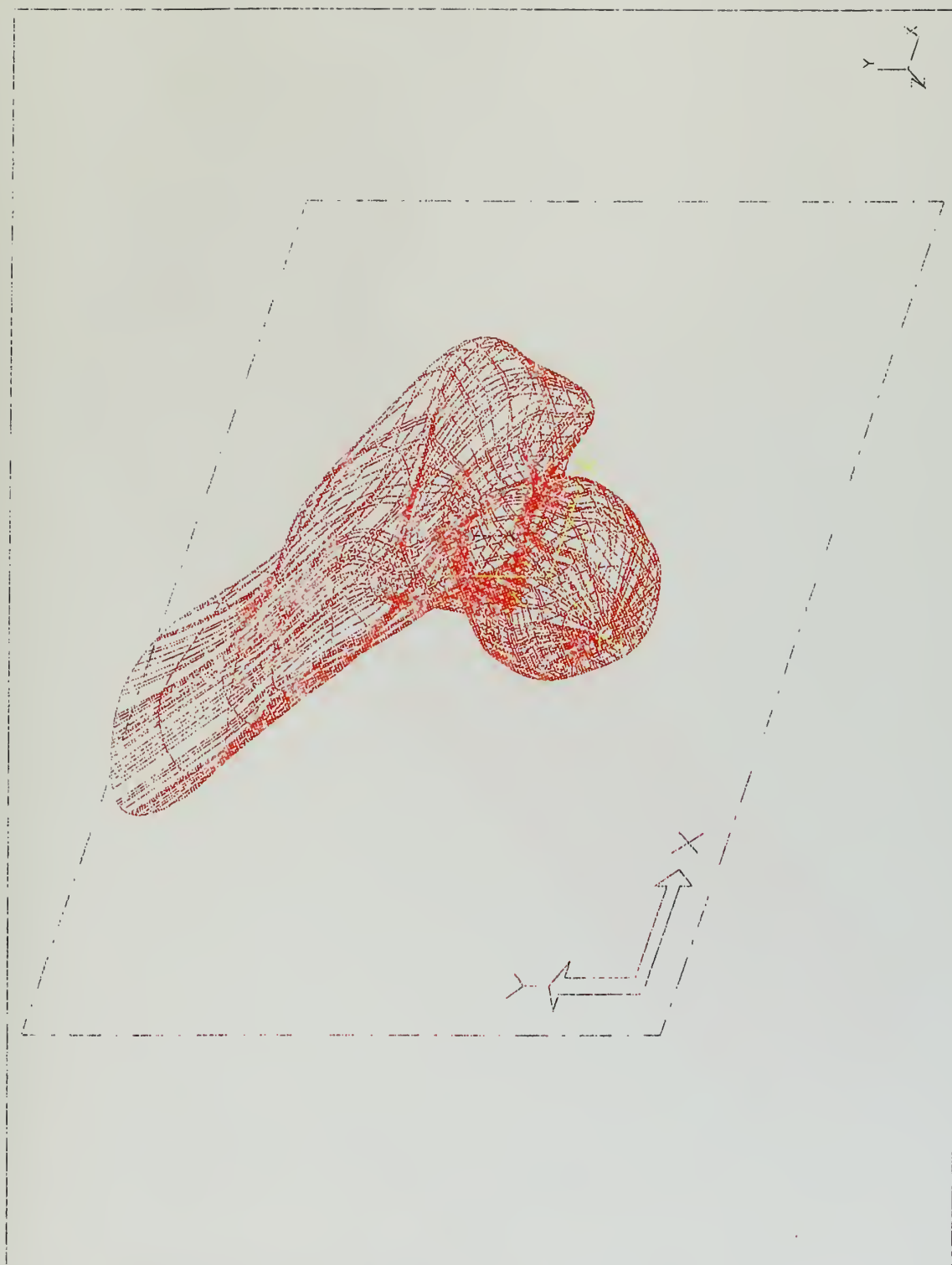
Figure 21: Circular planes.

26

Figure 22: Outer Shell of the Femur after Lofting.
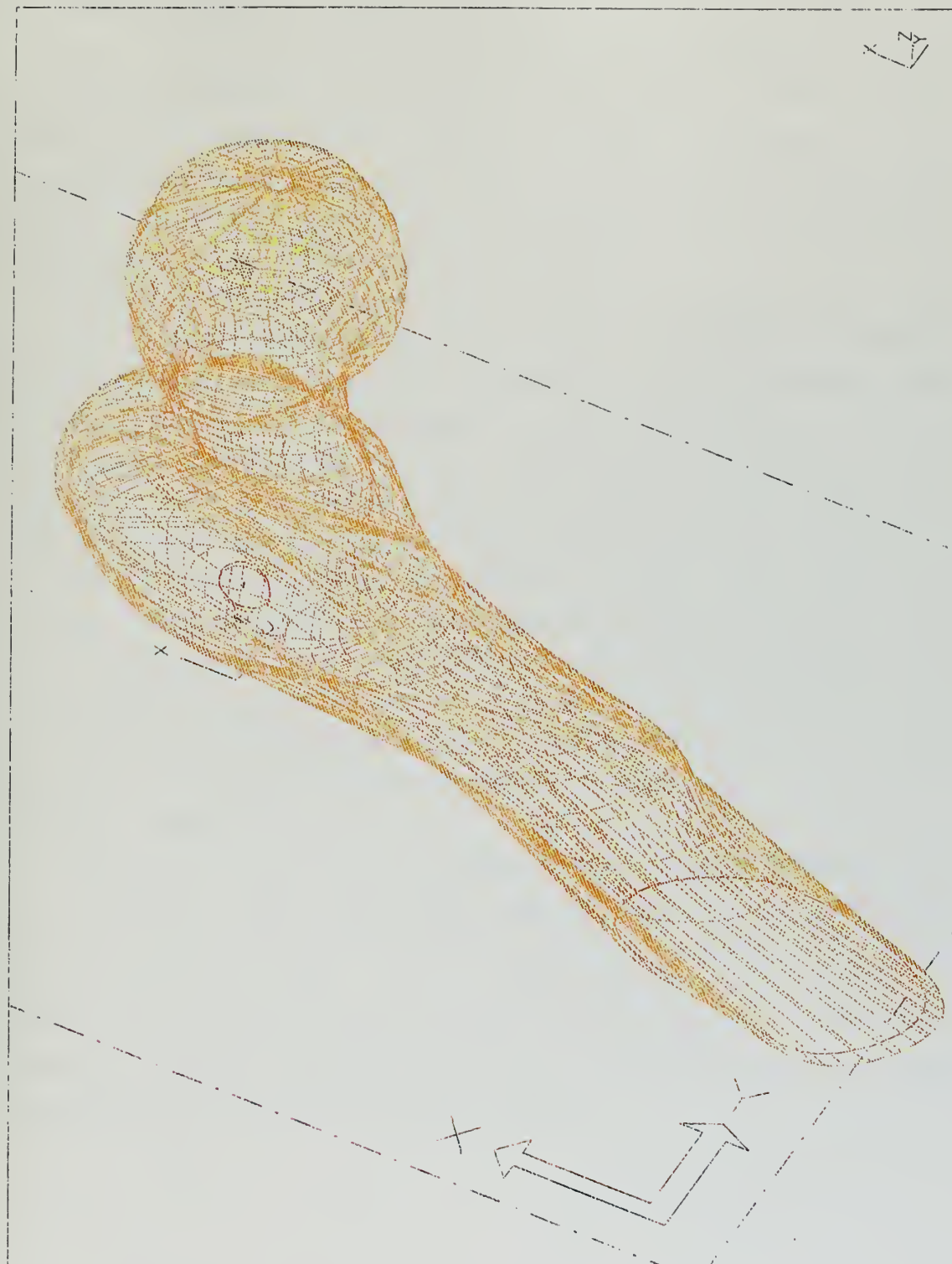
Figure 23: Hole at the Lesser Trochanter.

Figure 24: Hole at the Greater Trochanter.

B.   FINITE ELEMENT MODELING

The ideal model would have had a solid mesh with layers of varying physical and material properties. I-DEAS was not capable of producing so complex a mesh, therefore, shell elements were used instead to mesh the intact and core drilled femurs. The shell elements were defined to be quadrilateral elements with four nodes (Figures 25-27).

Once the finite element models were completed, physical and material properties were specified. The shell elements had an associated physical property which defined each elemental thickness to be eight millimeters. This dimension was chosen based on contour plots from Ref. 10, which indicates that the first eight millimeters, from the femur shell, are significantly stronger than the center portion of the femur. The material properties of the femur were also defined. These properties were thought to be anisotropic, but past studies have shown that these first eight millimeters are a homogenous, isotropic material [Ref. 11]. The elements of the model were assigned material properties with a Youngs Modulus of 5100MPa, Poisson's ratio of 0.3 and a density of 2000Kg/m^3 [Ref. 12 & 13].

Once the properties were established a quality mesh check was initiated. The mesh check has the ability to check the finite element models for errors that may have occurred during mesh definition [Ref. 14]. The program is capable of identifying modeling errors which include duplicate nodes and elements, missing elements and overly distorted elements. The program found no errors in the meshes.
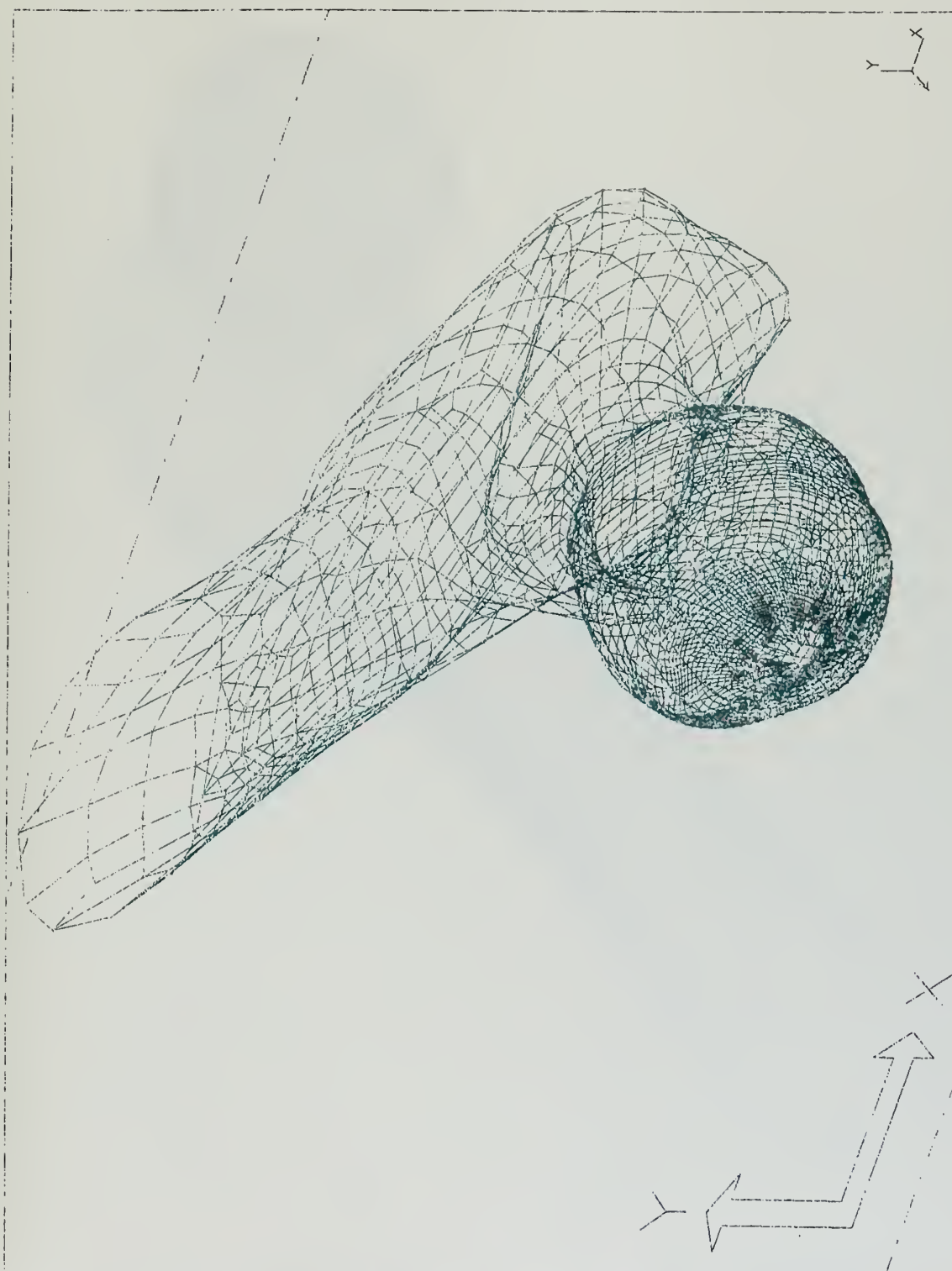
Figure 25: Meshed Intact Femur.

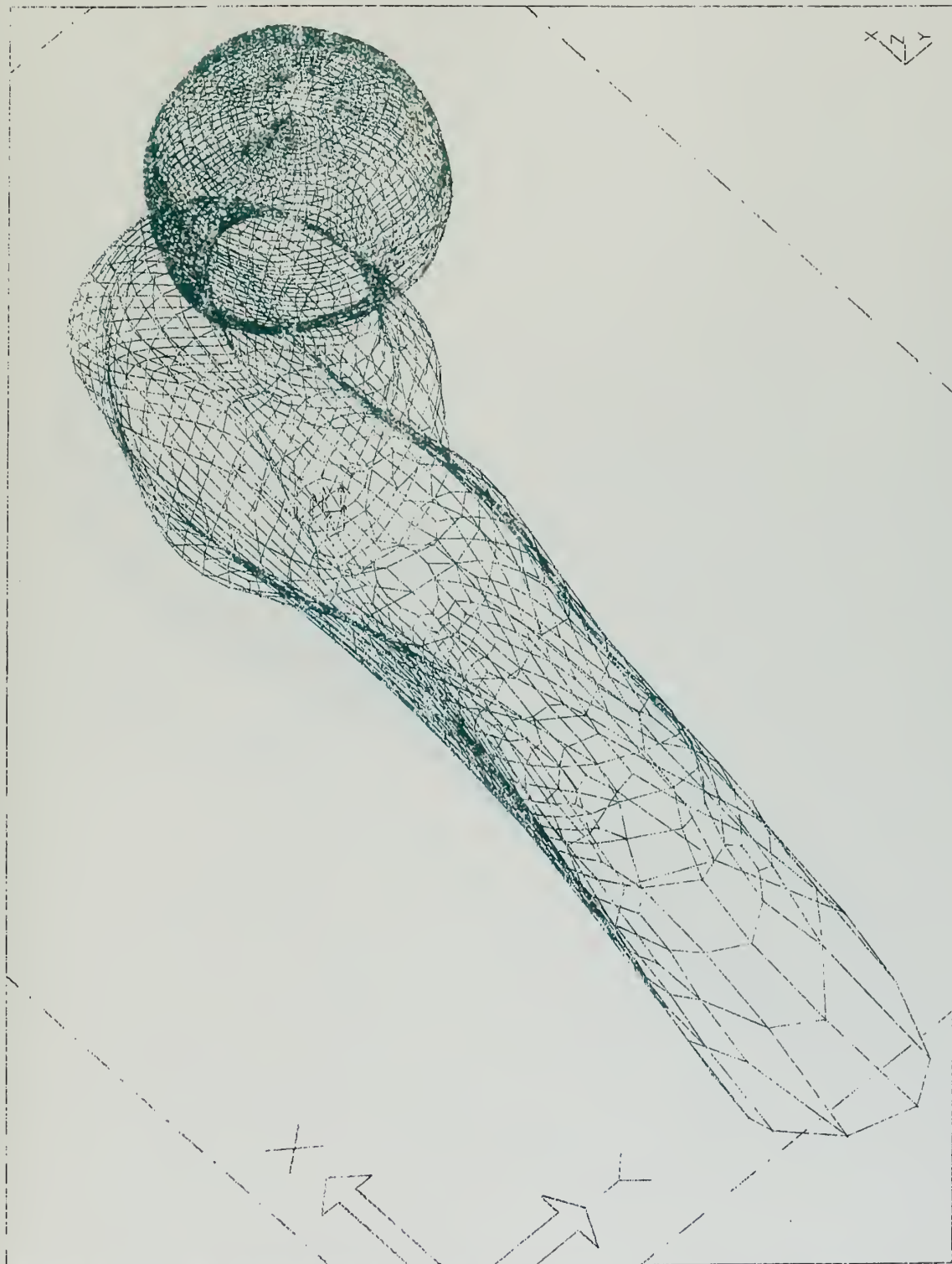Figure 26: Meshed Femur Core Drilled at Lesser Trochanter.

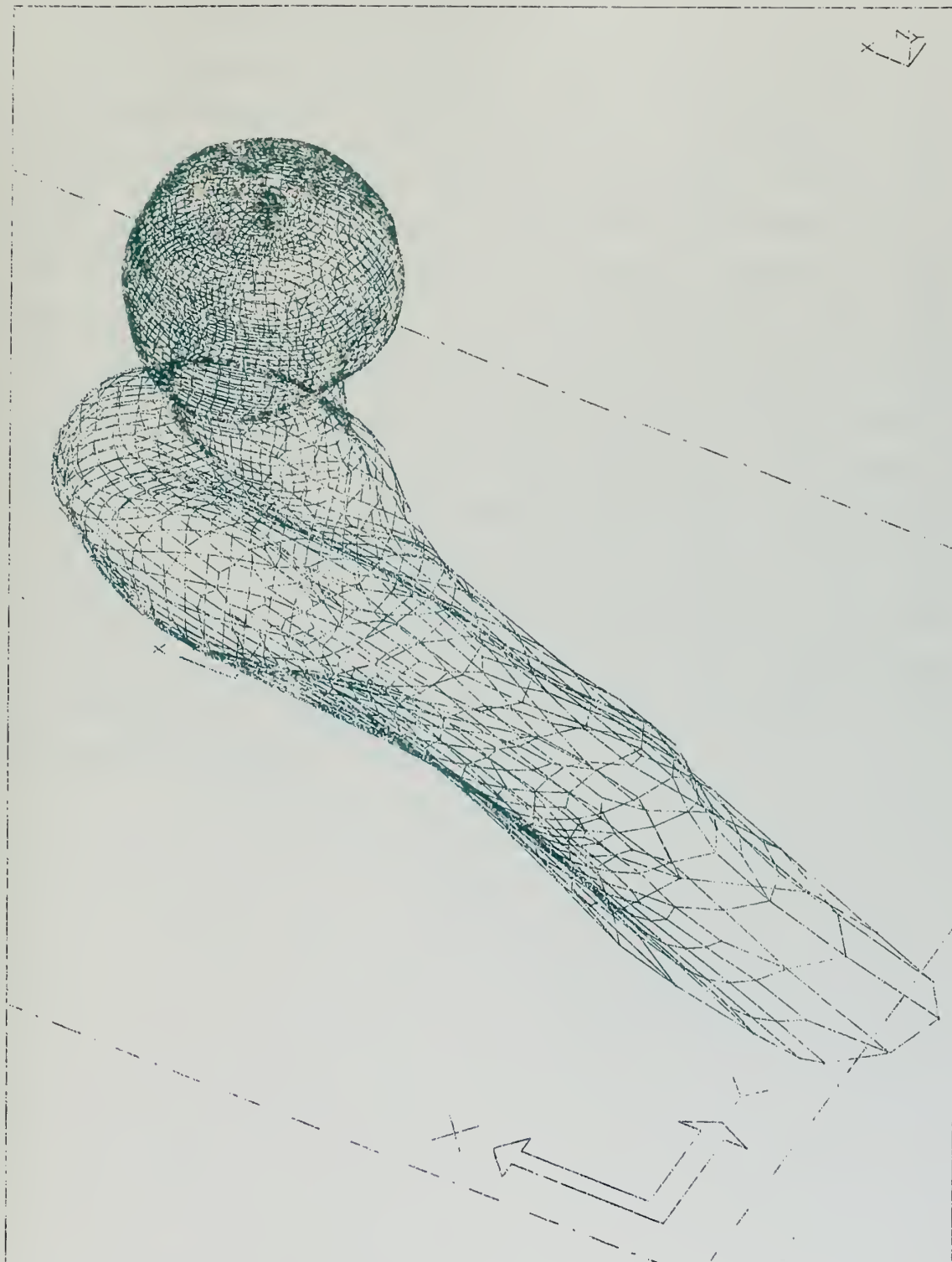Figure 27: Meshed Femur Core Drilled at Greater Trochanter.

33

C.   LOADING AND BOUNDARY CONDITIONS

Prior to solving the finite element model, boundary and loading conditions must be applied. The conditions in the lab for both static and dynamic analysis were duplicated in the computer model. Two static cases were analyzed. In the first static case, the distal end of the femur was clamped and a 5,000 Newton load was applied at superior margin of the femoral head (Figure 28). In the second static case the distal end was also clamped but rollers were added at the femoral head to simulate the rolling action of the head in the hip socket. A 5,000 Newton load was applied at the greater trochanter to simulate a lateral fall (Figure 29). The dynamic analysis was also given the boundary conditions of a clamped distal end and rollers at the femoral head (Figure 30). However, the loading condition was an impulse load with truncated triangular distribution of 5,000 Newtons over a time period of three milliseconds (Figure 31). This distribution approximates the force-time distribution, as shown in the experimental results in Figures 7-16
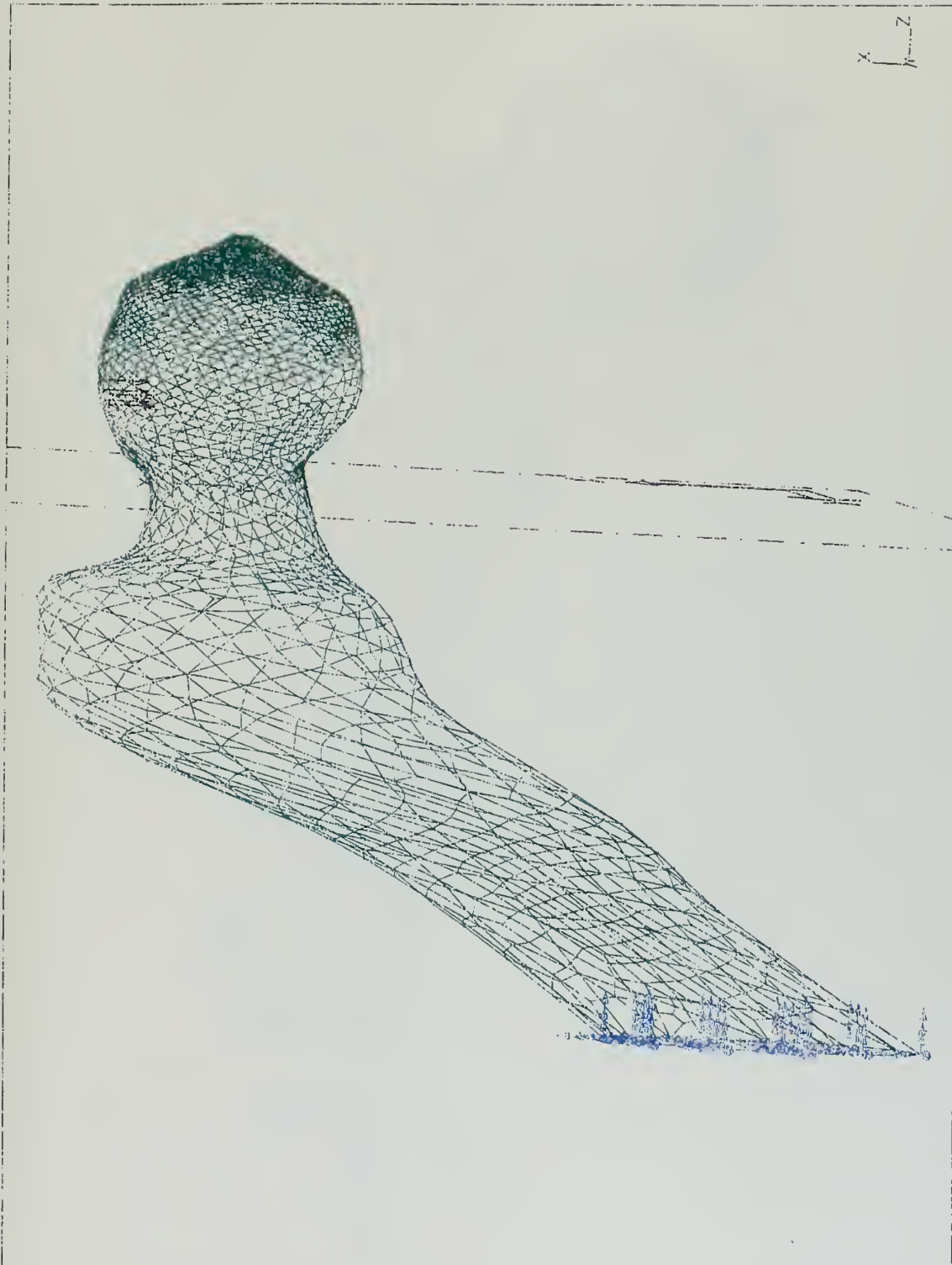
Figure 28: Loading and Boundary Conditions for First Static
Case.
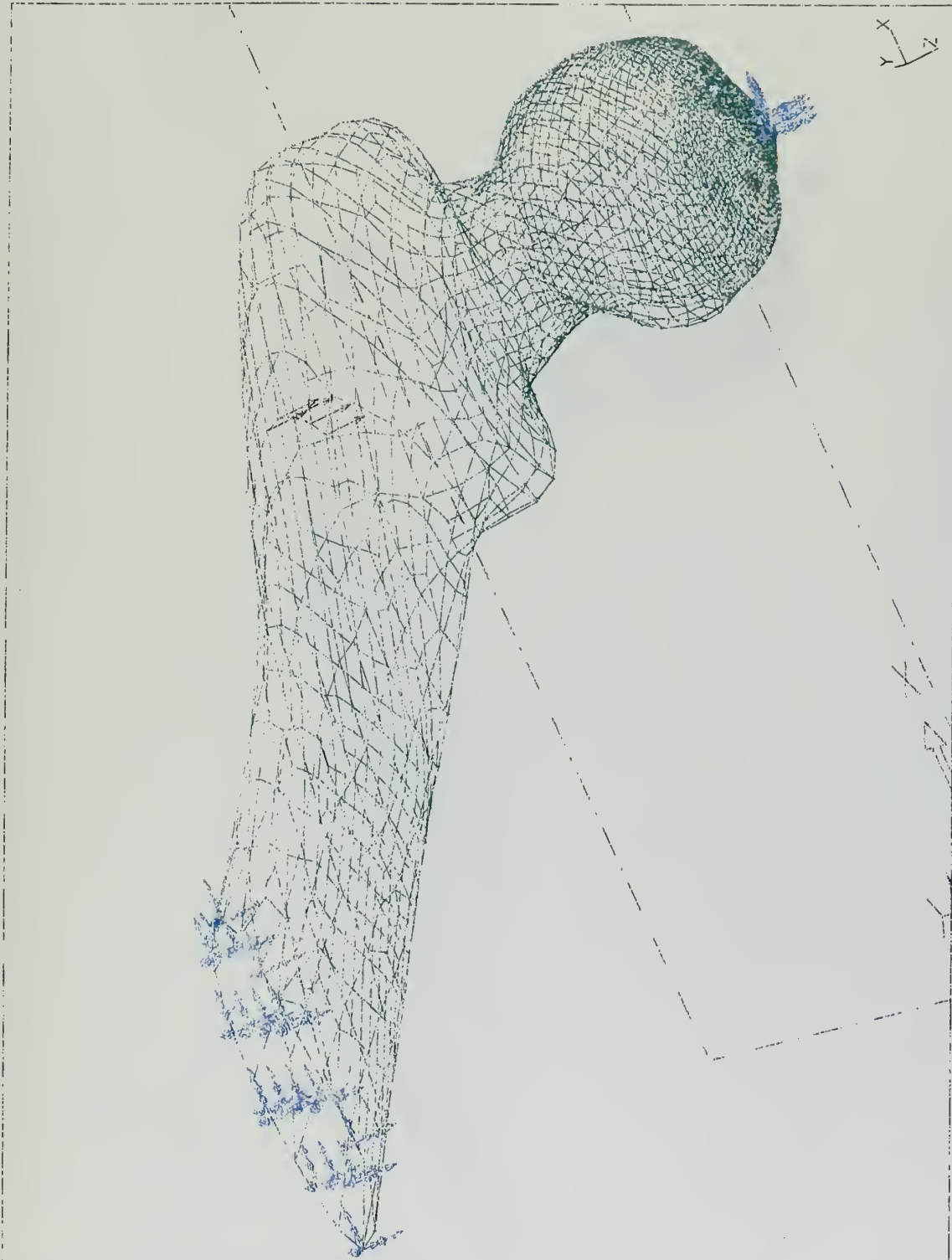
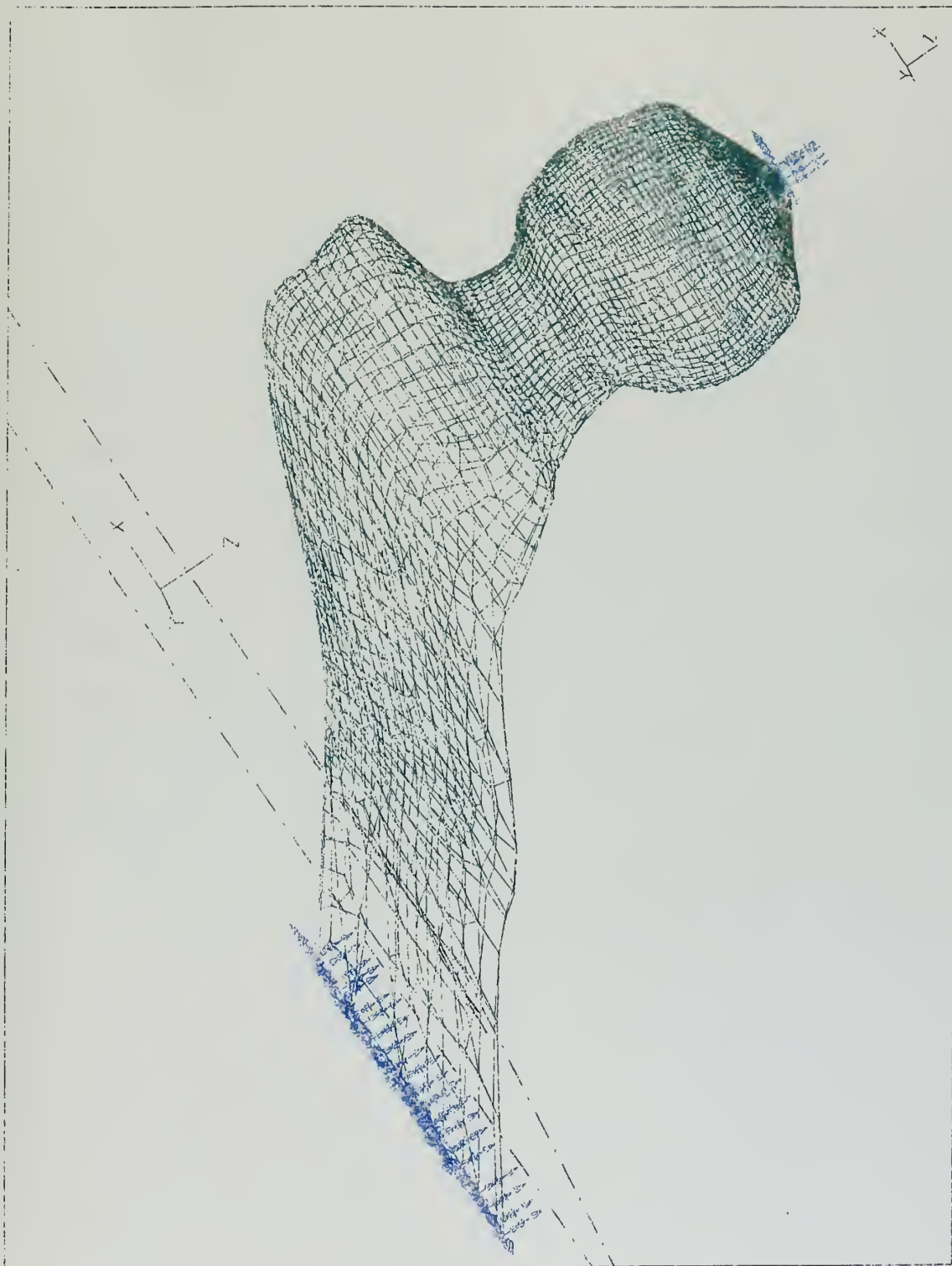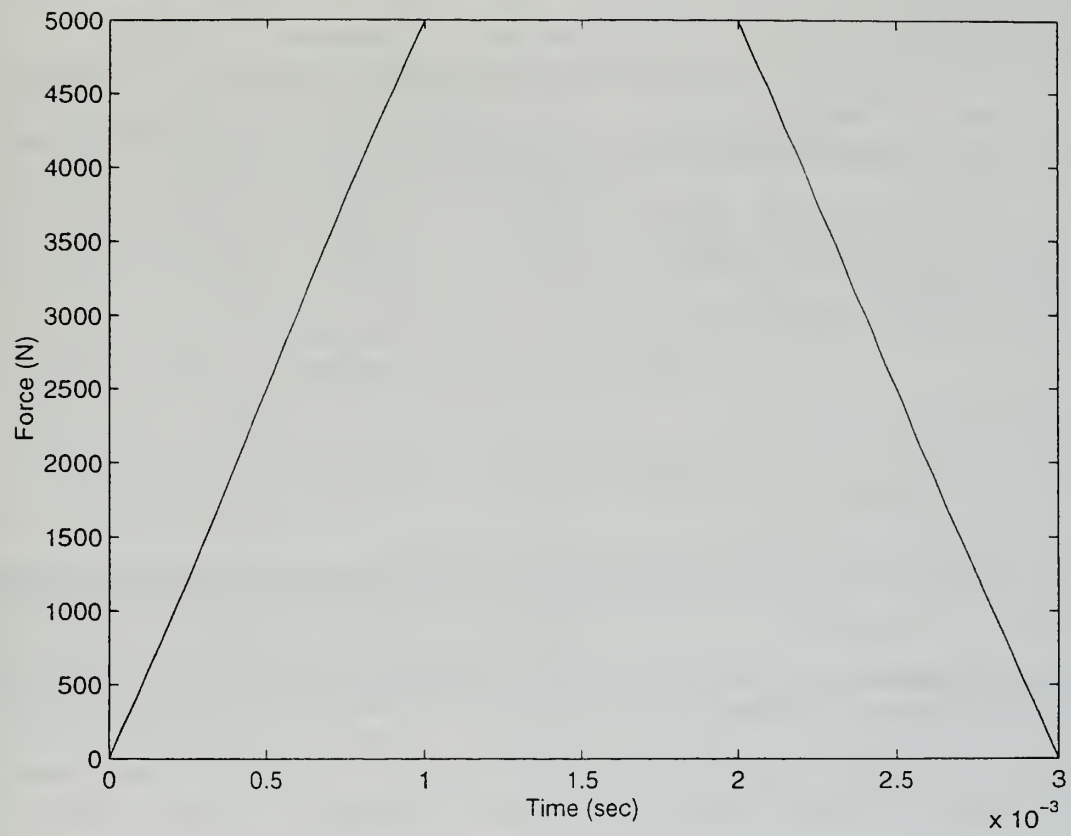Figure 29: Loading and Boundary Conditions for Second Static
Case.

Figure 30: Loading and Boundary Conditions for Dynamic Case.

Figure 31: Impulse Function.

D. NUMERICAL RESULTS

Upon completion of the static stress analysis for the eight models (Figures 32-39), Table 3 shows maximum stresses in the femur.

	No. of Nodes	No. of Elements	Maximum Stress
Loaded at Femoral Head			
Intact	3679	3667	68.7 MPa
Core Drilled at Lesser Trochanter (10mm)	4986	4971	77.9 MPa
Core Drilled at Greater Trochanter (10mm)	4164	4151	71.5 MPa
Core Drilled at Greater Trochanter (12mm)	4550	4537	77.9 MPa
Load at Greater Trochanter			
Intact	3679	3667	42 MPa
Core Drilled at Lesser Trochanter (10mm)	4986	4971	74.1 MPa
Core Drilled at Greater Trochanter (10mm)	4164	4151	54.7 MPa
Core Drilled at Greater Trochanter (12mm)	4550	4537	57.7 MPa

Table 3: Maximum Stresses in Femur (Static Results).

It is not surprising that in both static loading cases intact
femurs experienced the least stress and larger diameter holes
produce larger stresses than smaller diameter holes. A core
drilled hole at the lesser trochanter yielded significantly
larger stresses than a core drilled hole at the greater
trochanter. The data also suggests that femurs loaded at the
femoral head exhibit higher stresses than femurs loaded at the
greater trochanter. A closer examination of core drilled
holes themselves, however, shows higher stresses around the
hole when loaded at the greater trochanter. Table 4 shows
maximum stresses around each core drilled hole.

	Max Stress Around Hole
Loaded at Femoral Head	
Core Drilled at Lesser Trochanter (10mm)	61.5 MPa
Core Drilled at Greater Trochanter (10mm)	50.4 MPa
Core Drilled at Greater Trochanter (12mm)	54.8 MPa
Loaded at Greater Trochanter	
Core Drilled at Lesser Trochanter (10mm)	68.7 MPa
Core Drilled at Greater Trochanter (10mm)	54.7 MPa
Core Drilled at Greater Trochanter (12mm)	57.7 MPa

Table 4: Maximum Stresses Around Hole (Static Results).

A comparison of the three core drilled holes of the two static cases indicate that femurs loaded at the greater trochanter exhibit higher stresses around the hole. This suggests that static testing should be conducted with the load at the greater trochanter in order to simulate a lateral fall. Not only does this give a more conservative analysis of stresses around the hole, but also produces a more realistic simulation of a femur fracture. Also, as before, larger diameter holes experience larger stresses and therefore the smallest diameter hole possible should be drilled. Finally, core drilled holes at the lesser trochanter do experience significantly higher stresses around the hole than core drilled holes at the greater trochanter. Obviously then, core drilling should if at all possible be done at the greater trochanter.

A dynamic analysis was performed using I-DEAS' finite-element code. The code uses modal decomposition techniques vice direct integration to solve for the stresses. The decomposition technique approximates the distributed mass system with a finite number of lumped masses. The lumped masses are then connected to each other by elastic and damping members. The matrix equations of motion used to approximate the continuous system can be written:

$$[M]\ddot{x}(t) + [C]\dot{x}(t) + [K]x(t) = F(t) \qquad \textbf{(2)}$$

where,

$[M]$ = Mass Matrix
$[K]$ = Stiffness Matrix
$[C]$ = Damping Matrix
$x(t)$ = Displacement Vector
$\dot{x}(t)$ = Velocity Vector
$\ddot{x}(t)$ = Acceleration Vector
$F(t)$ = Force Vector

Equation 2 represents a set of "n" coupled equations. Solving for the associated eigenvalues and using the principle of orthogonality allows these coupled equations to be written as a set of "n" uncoupled equations as follows:

$$\ddot{q}(t) + [\eta_i \omega_i]\dot{q}(t) + [\omega_i^2]q(t) = f(t) \qquad (3)$$

where,

$$x(t) = [\phi]q(t) \qquad (4)$$

$$f(t) = [\phi]^T F(t) \qquad (5)$$

$[\Phi]$ = Eigenvector Matrix
$q(t)$ = Modal Position Vector
$\dot{q}(t)$ = Modal Velocity Vector
$\ddot{q}(t)$ = Modal Acceleration Vector
$[\eta_i \omega_i]$ = Diagonal Modal Damping Matrix
$[\omega_i^2]$ = Diagonal Modal Frequency Matrix
η_i = Modal Loss Factor
$f(t)$ = Modal Force Vector

Also, the forcing function is the impulse function, as shown in Figure 31. Each of the uncoupled equations of motion can now be solved independently and the total system response is determined by summing up each individual response. With displacement now known strains can be obtained. From strains and the material constitutive equation stresses can be calculated.

Because I-DEAS uses modal decomposition, only the first twenty modes could be analyzed for the dynamic stresses due to computer storage limitations. Results of dynamics stress analysis are given in Figures 40 and 41. Table 5 shows the maximum dynamic stresses in the femur and around the hole.

|	No. of Nodes	No. of Elements	Maximum Stress in the Femur	Maximum Stress Around the Hole
Intact	3679	3667	33.8 MPa	
Core Drilled at Lesser Trochanter (10mm)	5008	4993	49.5 MPa	34.8 MPa

Table 5: Dynamic Stress Results.

The dynamic data also shows that femurs that are core drilled exhibit higher stresses than intact femurs. A comparison of the dynamic and static data shows lower stresses in the dynamic case. One would expect dynamic stresses to exceed static stresses. It is believed that since only twenty modes were analyzed, the dynamic stresses were not accurately represented. To get a more accurate representation of the stress field more higher mode shapes have to be included or a different finite-element code that utilizes a direct time integration technique may be used to solve for the stresses.
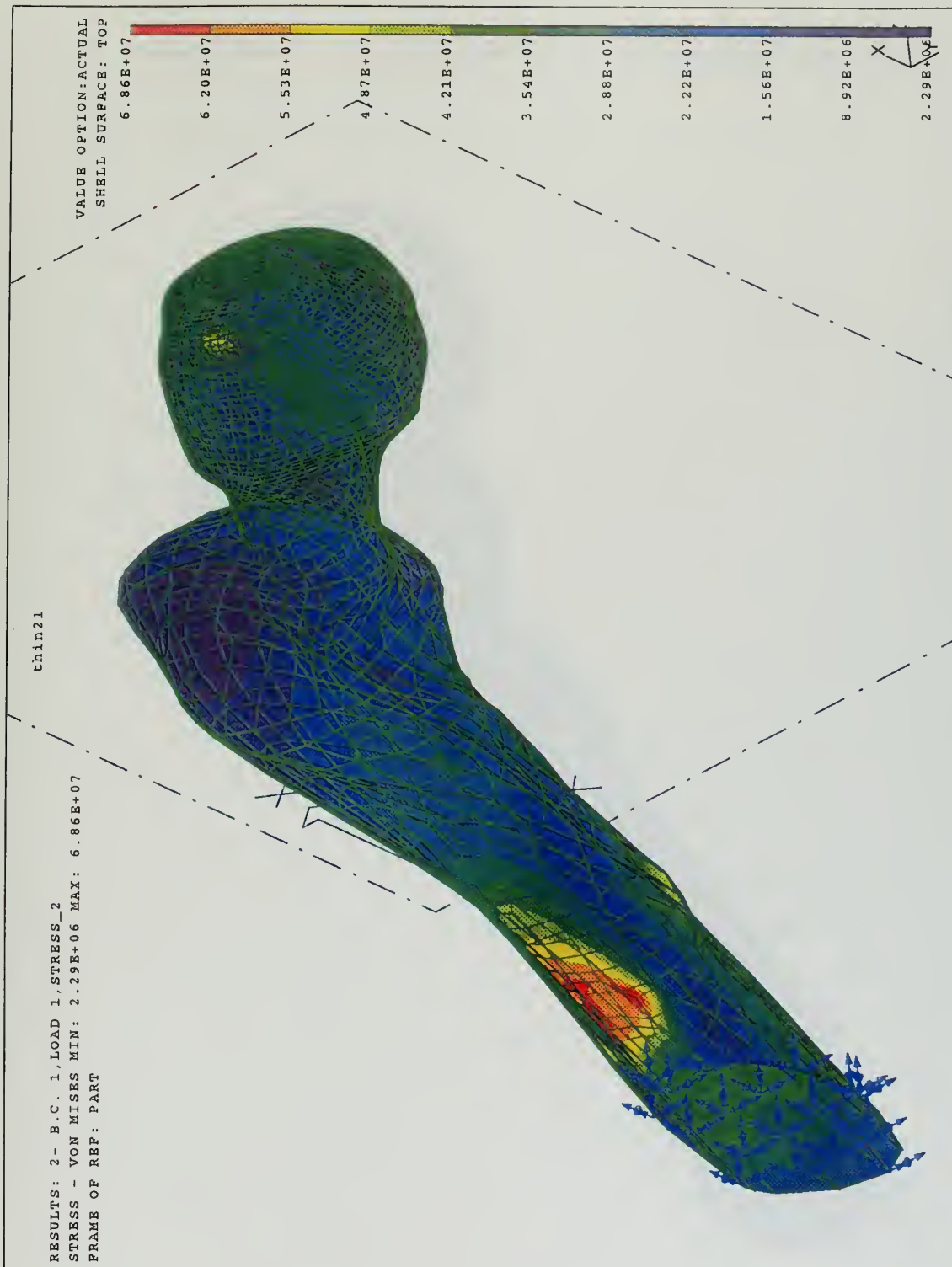
Figure 32:   Static Stresses for Intact Femur Loaded at the Femoral Head.

44
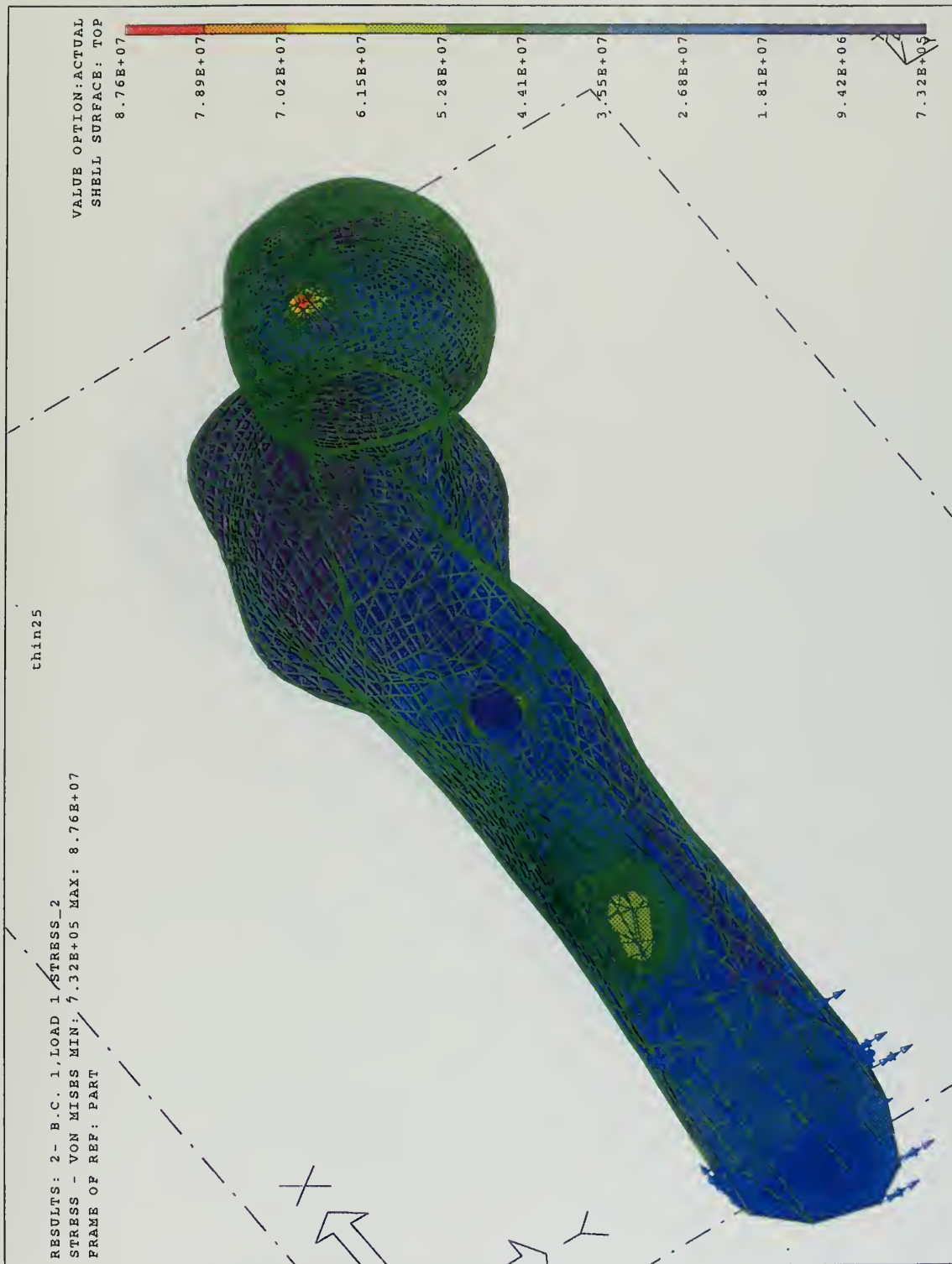
Figure 33: Static Stresses for Core Drilled Femur at the Lesser Trochanter (10mm) and Loaded at the Femoral Head.
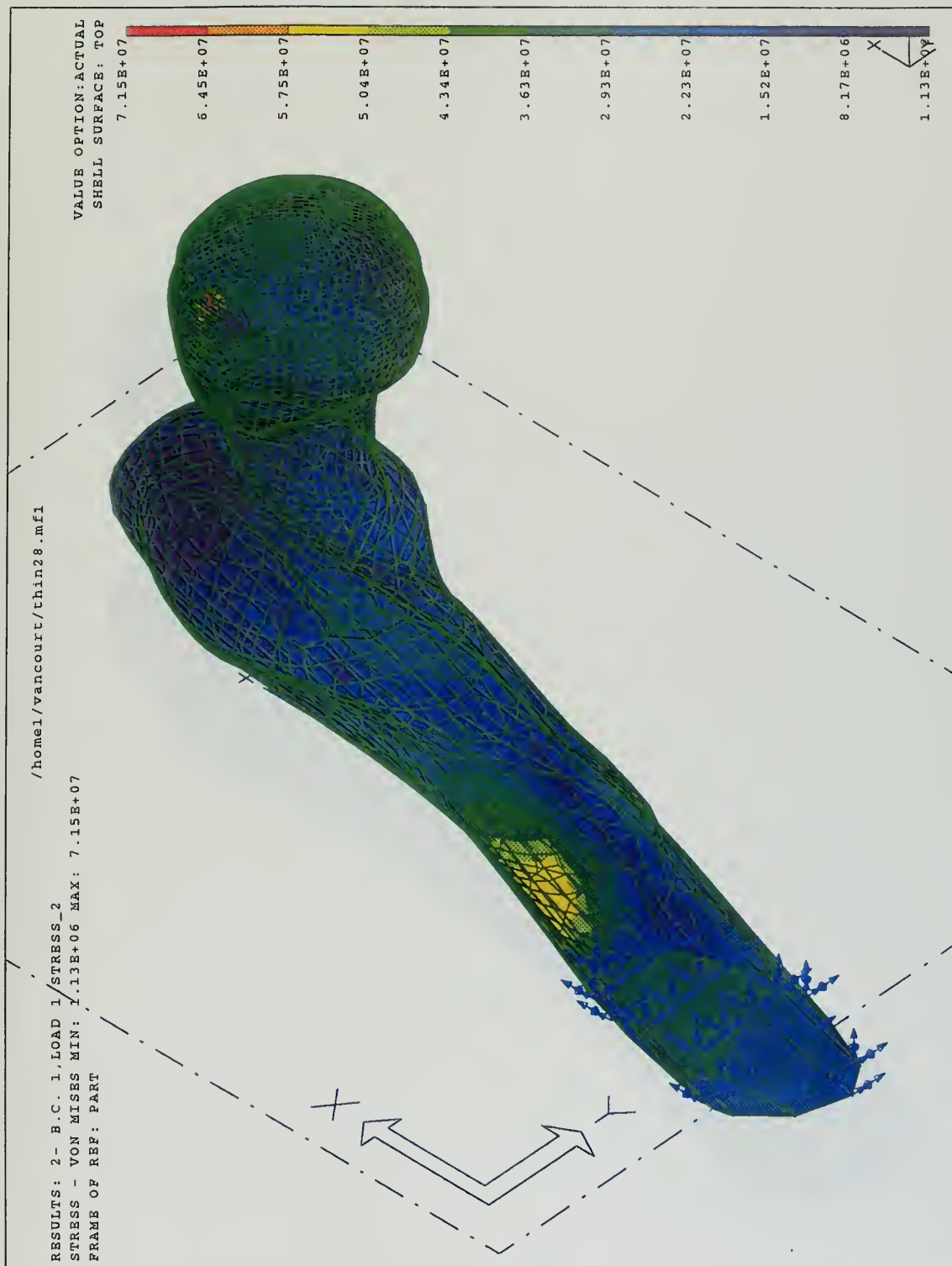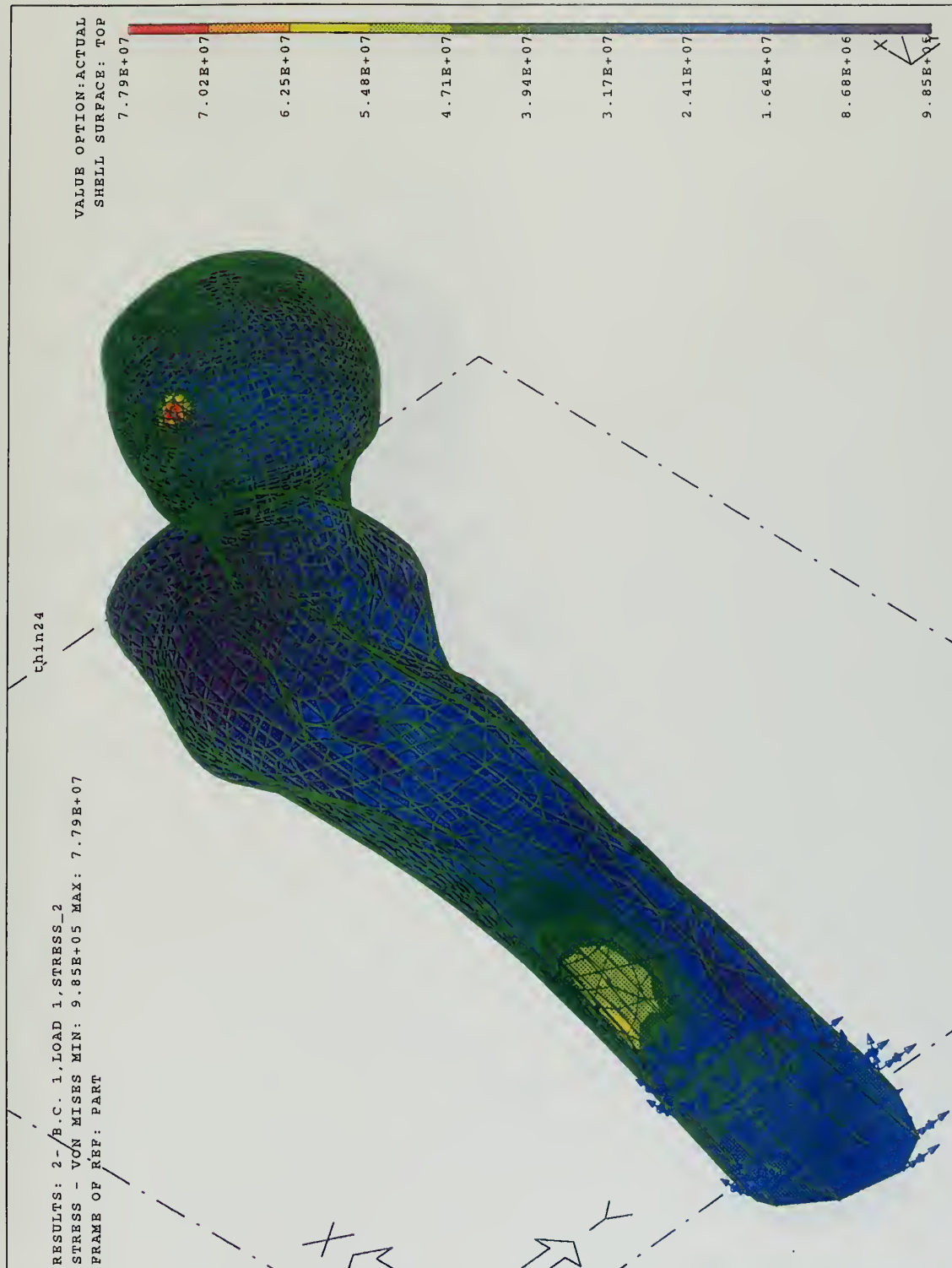
Figure 34: Static Stresses for Core Drilled Femur at the Greater Trochanter (10mm) and Loaded at the Femoral Head.

Figure 35: Static Stresses for Core Drilled Femur at the Greater Trochanter (12mm) and Loaded at the Femoral Head.
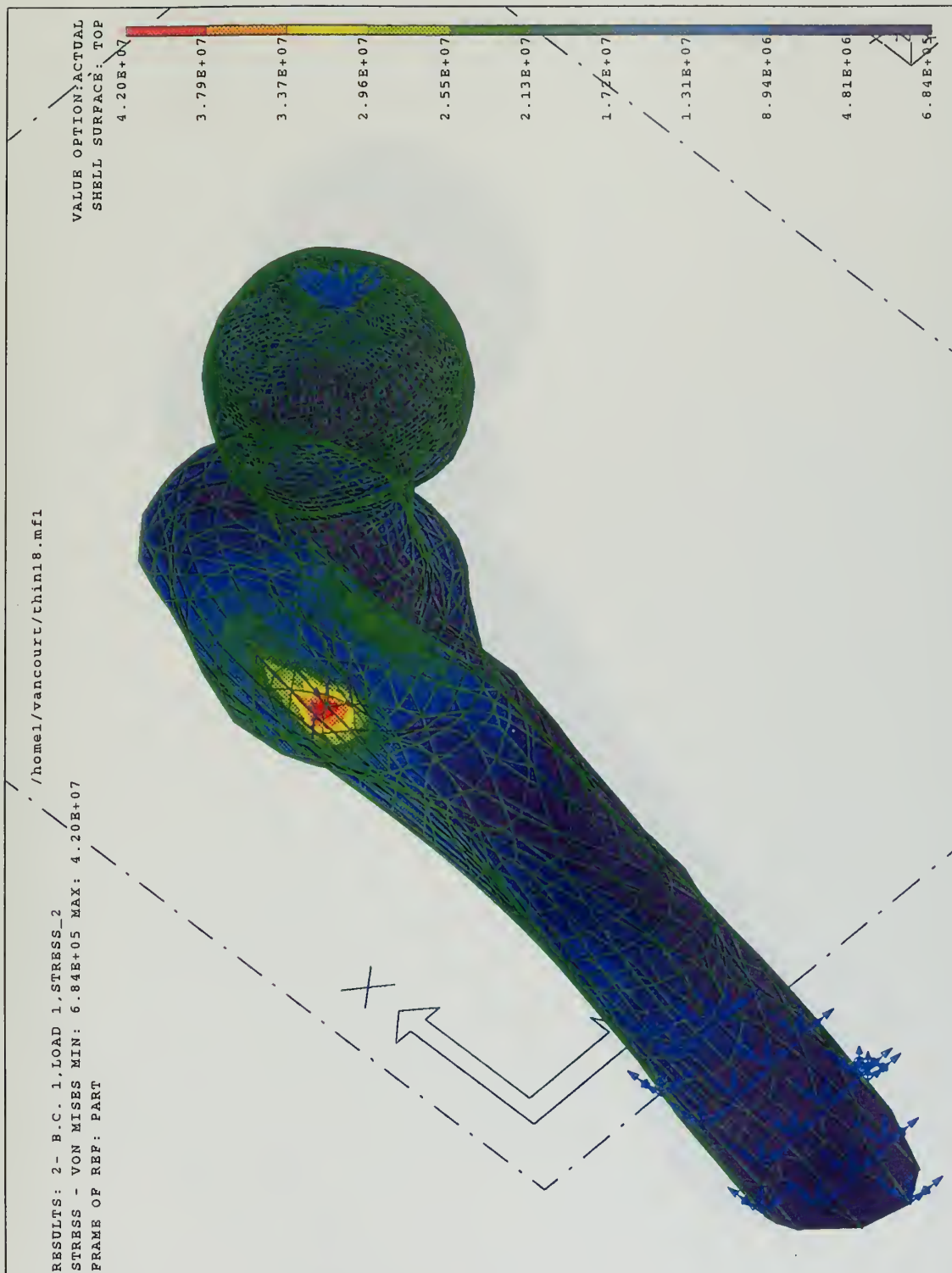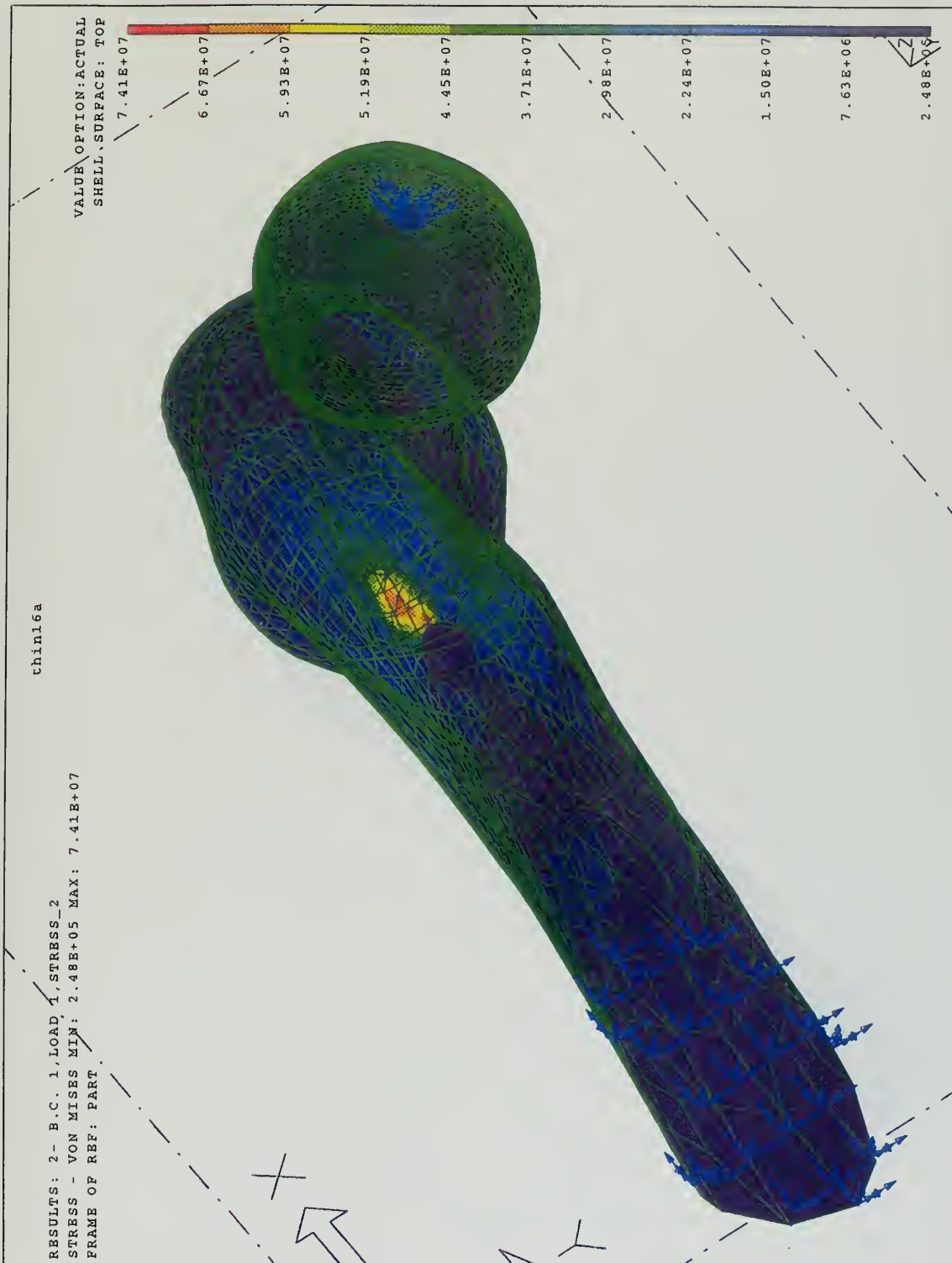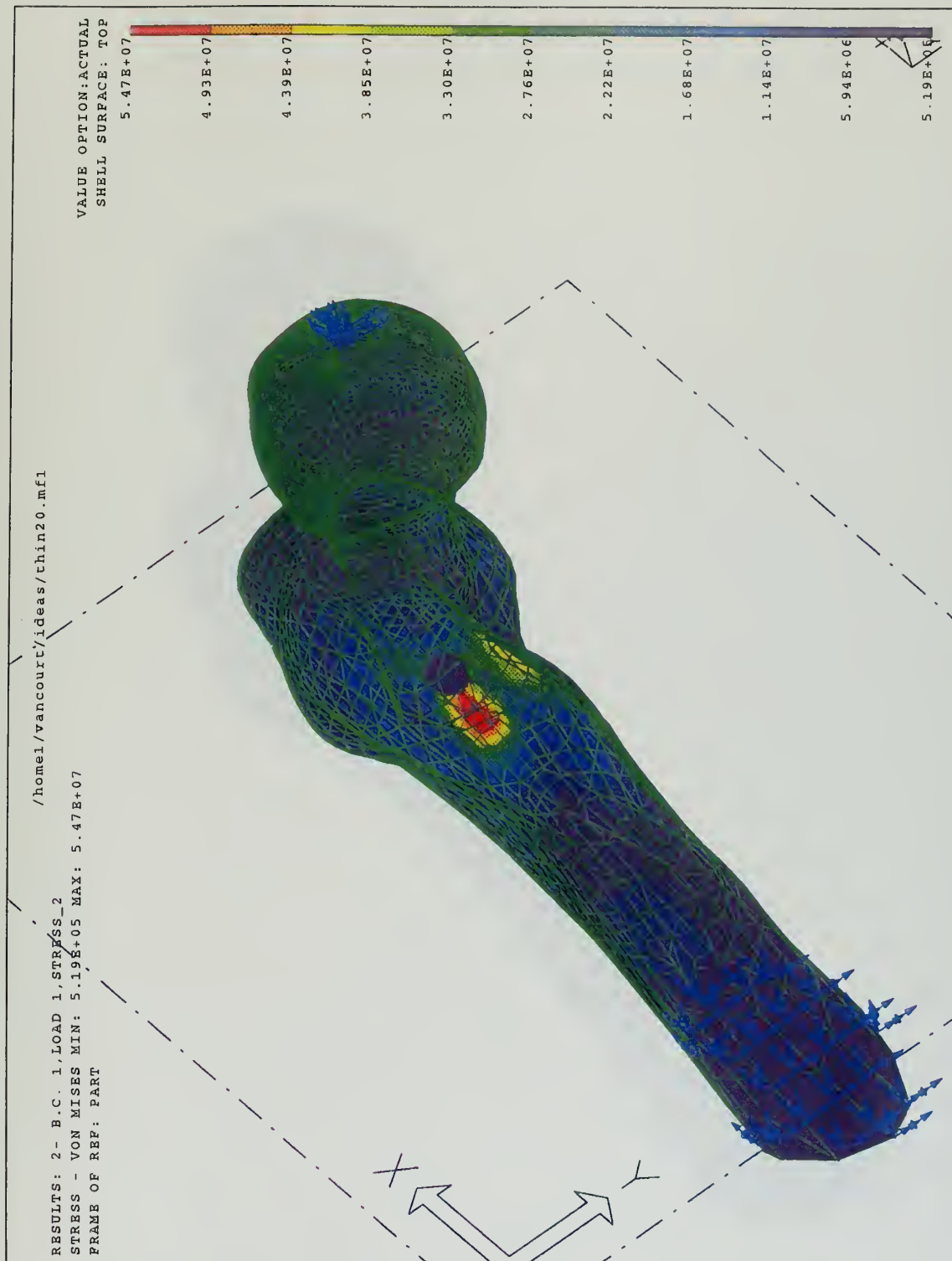
Figure 36: Static Stresses for Intact Femur Loaded at the Greater Trochanter.

Figure 37: Static Stresses for Core Drilled Femur at the Lesser Trochanter (10mm) and Loaded at the Greater Trochanter.

Figure 38: Static Stresses for Core Drilled Femur at the Greater Trochanter (10mm) and Loaded at the Greater Trochanter.
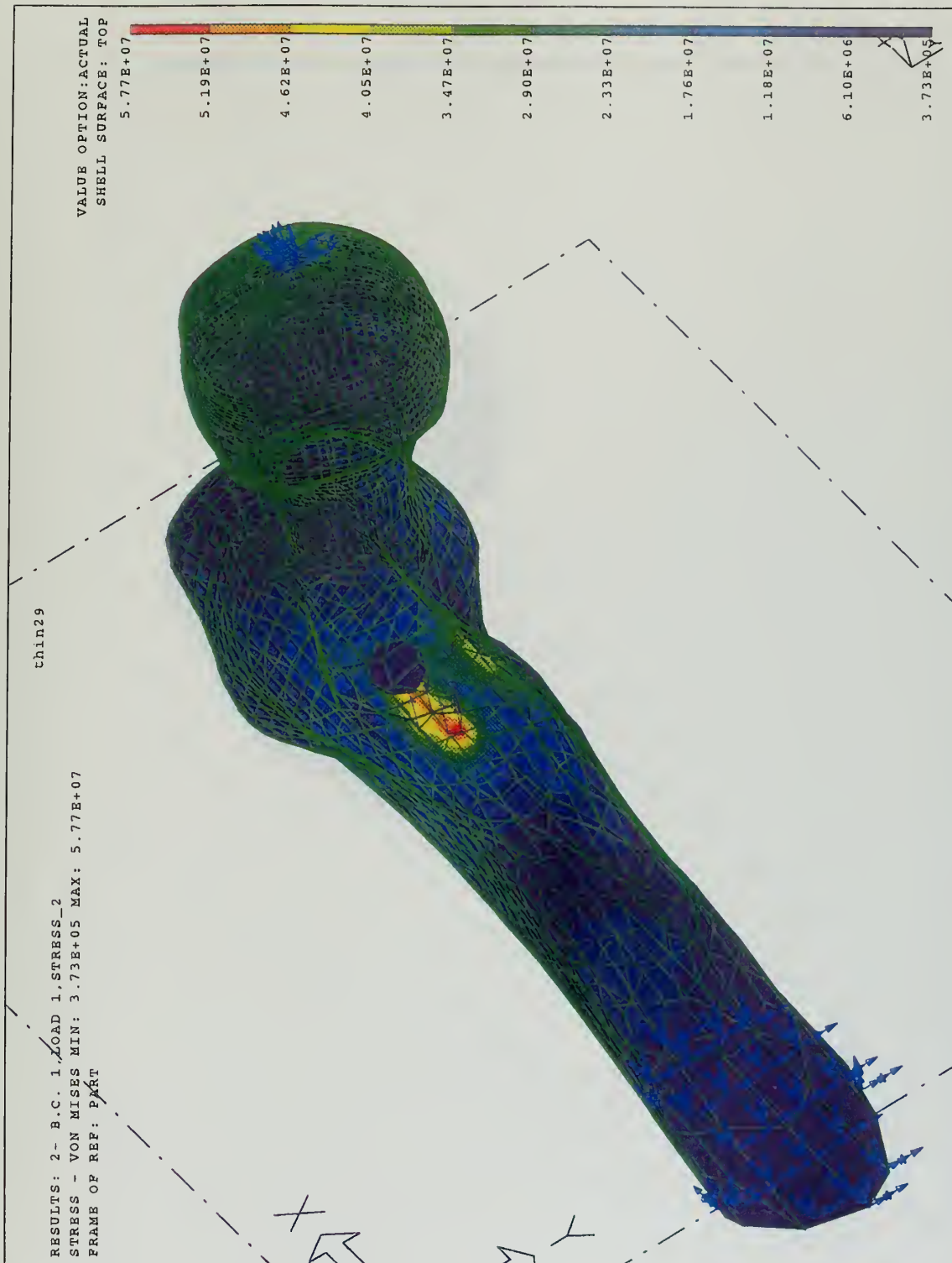
Figure 39: Static Stresses for Core Drilled Femur at the Greater Trochanter (12mm) and Loaded at the Greater Trochanter.
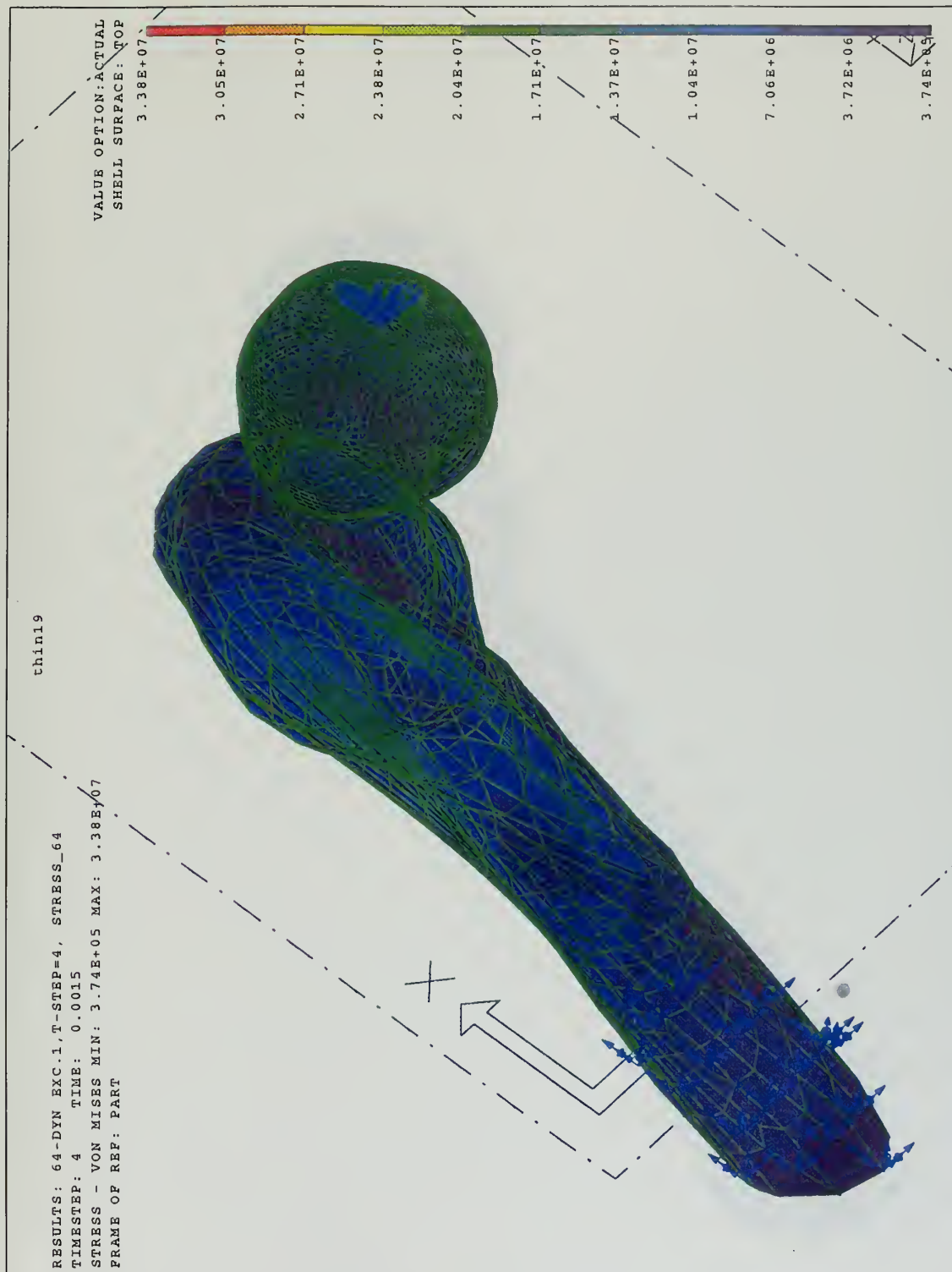
Figure 40: Dynamic Stresses for Intact Femur Loaded at the
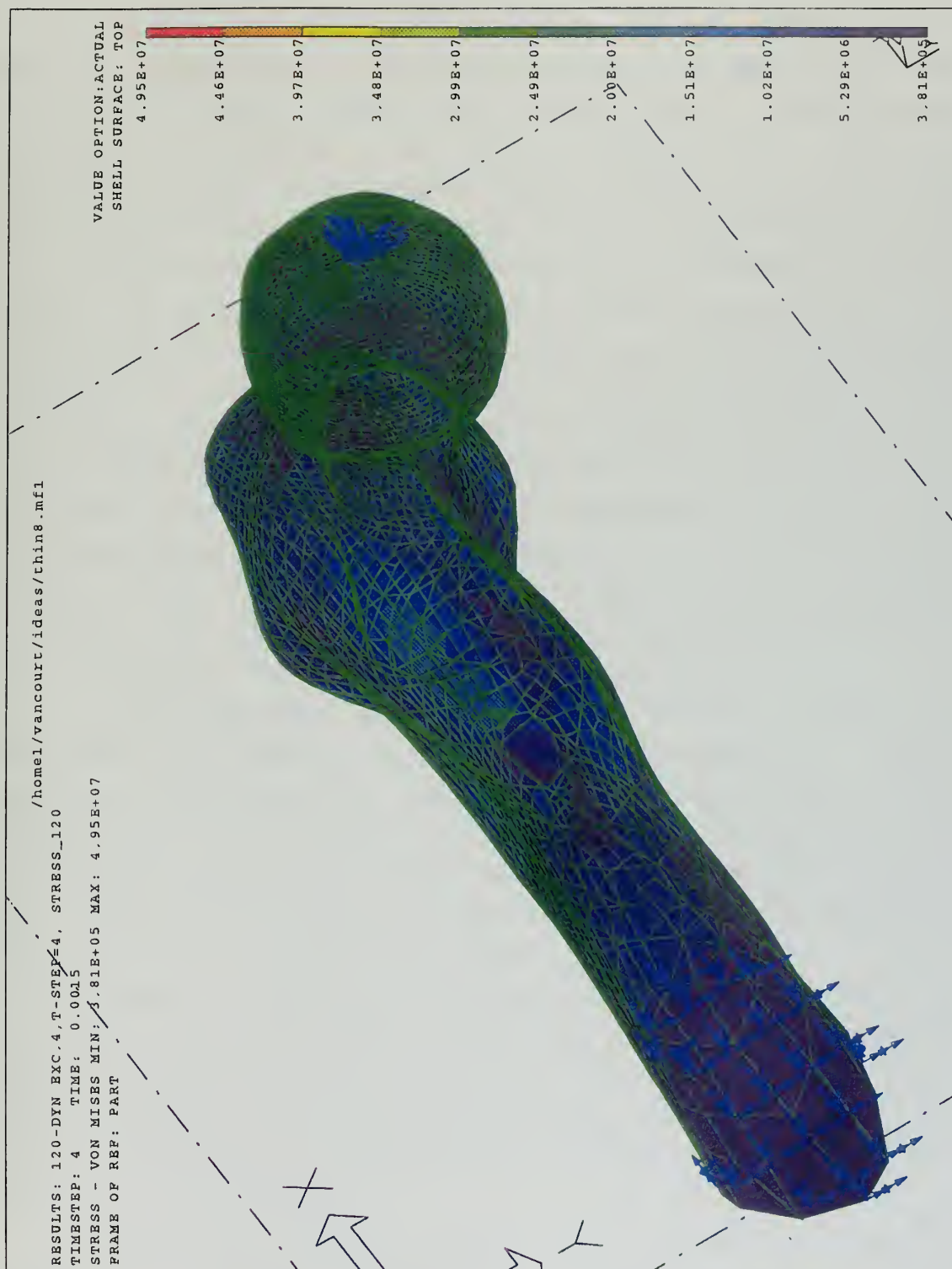Greater Trochanter.

Figure 41: Dynamic Stresses for Core Drilled Femur at the Lesser Trochanter (10mm) and Loaded at the Greater Trochanter.

V. CONCLUSIONS

Due to individual differences in femurs, matched sets must be utilized when comparing failure loads for intact and core drilled femurs. The three matched sets of femurs were fractured dynamically and the results, as expected, demonstrated that core drilled femurs failed at a lower load than intact femurs. A comparison of the experimental static and dynamic results, however, show very different fracture patterns of the femurs. The static results showed that all six femurs, intact and core drilled, had intertrochanteric fractures. The dynamic results, which provide a more realistic simulation of a lateral fall, showed that the three core drilled femurs suffered intertrochanteric fractures while the seven intact femurs had five subtrochanteric and two pertrochanteric fractures. In conclusion, dynamic impact testing is recommended when performing future fracture testing of femurs. Not only does this give more accurate simulation but it produces true fracture patterns of femurs.

A finite-element analysis of the proximal femur was developed to augment the experimental results. Three different conditions of the femur were examined: loaded dynamically at the greater trochanter, loaded statically at the greater trochanter, and loaded at the superior marginal head. Core drilled holes with various sizes and locations on the trochanter were also examined.

A dynamic analysis was done and these results were consistent with the static results in that the core drilled femur developed greater stresses than the intact femur. Because I-DEAS uses modal decomposition techniques and only twenty modes could be analyzed, the dynamic stresses were not accurately represented.

In comparing the two static cases, when the load is located at the superior marginal head greater stresses in the femur are developed than when it is loaded at the greater

trochanter. However, greater stresses are developed around the hole when the femur is loaded at the greater trochanter. This is a more conservative analysis of stress around the hole and the conditions are more realistic. Core drilled femurs were analyzed with two different hole sizes, ten and twelve millimeters. The results, as expected, yielded that larger diameter holes developed larger stresses than smaller diameter holes. For the same hole size, core drilled holes at the lesser trochanter developed stresses that are over twenty percent higher than core drilled holes at the greater trochanter.

This first generation finite-element analysis suggests that the hole should be as small as possible and be located at the greater trochanter. Further, when conducting experiments in the lab, the load should be located at the greater trochanter vice the superior marginal head of the femur.

VI. RECOMMENDATIONS

When comparing failure loads of intact and core drilled femurs, matched sets of femurs should be utilized.

The graphics portions of I-DEAS is excellent and recommended for continued use. In addition, the finite element analysis of static stresses in I-DEAS is recommended. However, because I-DEAS uses modal decomposition techniques to solve for the dynamic stresses, another finite-element code that utilizes direct time integration to solve for the dynamic stresses is recommended. I-DEAS has the capability of exporting and importing files. So, construct the femur in I-DEAS and transport to another finite-element code for the solution.

Finally, to achieve even more accurate finite element results, a solid mesh of the femur is desired. Based on contour plots from Ref. 15, the entire physical and material properties are known, for the three dimensional model. However, due to the complex geometry very small elements will have to be used, creating many solid elements. With so many elements computer memory and time will be a concern. As a result, an optimum meshing technique is needed.

LIST OF REFERENCES

1. Courtney, A. C., Wachtel, E. P., Myers, E. R., and Hayes, W.C.: Age-Related Reductions in the Strength of the Femur Tested in a Fall-Loading Configuration, Vol. 77-A, No. 3., March 1995, pp. 387-395.

2. Jacues, A.: Nontraumatic Avascular Necrosis of the Femoral Head Past, Present and Future, March 1991, pp. 12-14.

3. Baker, K. J., Brown, T. D., and Brand R. A.: A Finite-Element Analysis of the Effects of Intertrochanteric Osteotomy on Stresses in Femoral Head Osteonecrosis, May 1989, pp. 183-198.

4. Brown, T. D., Way, M. E., and Ferguson, A. P.: Mechanical Characteristics of the Bone in Femoral Capital Aseptic Necrosis. Clin. Orthop. 156:240, 1981.

5. Favenesi, J. A., Gardeniers, J. W. M., Huiskes, R., and Slooff, T. J.: Mechanical Properties of Normal and Avascular Cancellous Bone. *In* Ducheyne, P., Van Der Perre, G., and Aubert, A. E. (eds.): Biomaterials and Biomechanics 1983. Amsterdam, Elsevier, 1984, pp. 121-126.

6. Courtney, A. C., Wachtel, E. P., Myers, E. R., and Hayes, W.C.: Age-Related Reductions in the Strength of the Femur Tested in a Fall-Loading Configuration, Vol. 77-A, No. 3., March 1995, pp. 387-395.

7. Oh, I, and Harris, W. H.: Proximal Strain Distribution in the Loaded Femur, J Bone and Joint Surgery, Vol. 60-A, No. 1, January 1978, pp. 75-85.

8. Backman, S.: *The Proximal End of the Femur*, 1957, pp. 136.

9. Lawry, M. H., I-DEAS *Student Guide*, pp. 254, Structural Dynamics Research Corporation, 1993.

10. Brown, T. D., and Ferguson, A. B.: Mechanical Property Distributions in the Cancellous Bone of the Human Proximal Femur, Acta Orthop. Scand. 51, 1980, pp. 429-437.

11. Brown, T. D., and Ferguson, A. B.: Mechanical Property Distributions in the Cancellous Bone of the Human Proximal Femur, Acta Orthop. Scand. 51, 1980, pp. 429-437.

12. Brown, T. D., and Ferguson, A. B.: Mechanical Property Distributions in the Cancellous Bone of the Human Proximal Femur, Acta Orthop. Scand. 51, 1980, pp. 429-437.

13. van Riebergen, B., Weinans, H., Huiskes, R., and Odgaard, A.: A New Method to Determine Trabecular Bone Elastic Properties and Loading Using Micromechanical Finite-Element Models, J Biomechanics, Vol. 28, No. 1, 1995, pp. 69-81.

14. Lawry, M. H., I-DEAS *Student Guide*, pp. 254, Structural Dynamics Research Corporation, 1993.

15. Brown, T. D., and Ferguson, A. B.: Mechanical Property Distributions in the Cancellous Bone of the Human Proximal Femur, Acta Orthop. Scand. 51, 1980, pp. 429-437.

GLOSSARY OF TERMS

ADDUCTION - Movement of part of the body towards midline.

ANTERIOR - Located in the front.

CANCELLOUS - Latticed or spongelike in structure.

DISTAL - Away from the center. Out toward the end. The hand is distal to the arm.

FEMUR - The thighbone, originating in the hip and extending down to the knee.

OSTEONECROSIS - Death of bone tissue.

POSTERIOR - Located in the back, or toward the rear.

PROXIMAL - Near the center of the body, as opposed to distal. The elbow is proximal to the wrist.

SAGITTAL - An anatomical term applied to the "front to back" plane of the body.

SUPERIOR - An anatomical term referring to an organ or part which is located above another organ or part of the body.

TRABECULA - A band of fibrous tissue which helps support the structure of a organ.

TROCHANTER - The prominence of the thighbone (femur) which can be felt below the hip region on the outer aspect of the upper thigh.

INITIAL DISTRIBUTION LIST

No. Copies

1. Defense Technical Information Center
   8725 John J. Kingman Rd., STE 0944
   Ft. Belvoir, VA 22060-6218

   2

2. Dudley Knox Library
   Naval Postgraduate School
   411 Dyer Rd.
   Monterey, CA 93943-5101

   2

3. Chairman, Code ME/Mc
   Department of Mechanical Engineering
   Naval Postgraduate School
   Monterey, CA 93940-5000

   1

4. Professor Young W. Kwon, ME/Kw
   Department of Mechanical Engineering
   Naval Postgraduate School
   Monterey, CA 93940-5000

   2

5. Naval/Mechanical Engineering, Code 34
   Naval Postgraduate School
   Monterey, CA 93940-5000

   1

6. LCDR Marlene DeMaio, MC, USNR
   Naval National Medical Center
   Department of Orthopedic Surgery
   8901 Wisconsin Ave.
   Bethesda, MD 20889-5000

   1

7. LT Ronald R. Van Court
   4833 W. Kaler Circle
   Glendale, AZ 85301

   3